

UNIVERSITI MALAYSIA PAHANG

BORANG PENGESAHAN STATUS TESIS♦

JUDUL: **AUTOMATED GUIDED VEHICLE (AGV) MODEL**

SESI PENGAJIAN: 2010/2011

Saya MOHD SHUKRI B ALIAS (881001-03-5727)
(HURUF BESAR)

mengaku membenarkan tesis (Sarjana Muda/~~Sarjana~~ /~~Doktor Falsafah~~)* ini disimpan di Perpustakaan dengan syarat-syarat kegunaan seperti berikut:

1. Tesis adalah hakmilik Universiti Malaysia Pahang (UMP).
2. Perpustakaan dibenarkan membuat salinan untuk tujuan pengajian sahaja.
3. Perpustakaan dibenarkan membuat salinan tesis ini sebagai bahan pertukaran antara institusi pengajian tinggi.
4. **Sila tandakan (√)

SULIT

(Mengandungi maklumat yang berdarjah keselamatan atau kepentingan Malaysia seperti yang termaktub di dalam AKTA RAHSIA RASMI 1972)

TERHAD

(Mengandungi maklumat TERHAD yang telah ditentukan oleh organisasi/badan di mana penyelidikan dijalankan)

TIDAK TERHAD

Disahkan oleh:

(TANDATANGAN PENULIS)

(TANDATANGAN PENYELIA)

Alamat Tetap:

LOT 1385 KG NILAM BARU 16010
KOTA BHARU KELANTAN

NORAZILA BT JAALAM
(Nama Penyelia)

Tarikh: **29 NOVEMBER 2010**

Tarikh: : **29 NOVEMBER 2010**

- CATATAN:
- * Potong yang tidak berkenaan.
 - ** Jika tesis ini SULIT atau TERHAD, sila lampirkan surat daripada pihak berkuasa/organisasi berkenaan dengan menyatakan sekali tempoh tesis ini perlu dikelaskan sebagai atau TERHAD.
 - ♦ Tesis dimaksudkan sebagai tesis bagi Ijazah doktor Falsafah dan Sarjana secara Penyelidikan, atau disertasi bagi pengajian secara kerja kursus dan penyelidikan, atau Laporan Projek Sarjana Muda (PSM).

**A STATOR RESISTANCE ESTIMATION OF INDUCTION
MOTOR USING NEURAL NETWORK**

MOHD SHUKRI BIN ALIAS

UNIVERSITY MALAYSIA PAHANG

**A STATOR RESISTANCE ESTIMATION OF INDUCTION
MOTOR USING NEURAL NETWORK**

MOHD SHUKRI BIN ALIAS

**A thesis submitted in partial fulfillment of the
requirements for the awarded of the Degree of Bachelor of Electrical &
Electronics Engineering**

**Faculty of Electrical & Electronics Engineering
University Malaysia Pahang**

NOVEMBER, 2010

I declare that this thesis entitled “A STATOR RESISTANCE ESTIMATION OF INDUCTION MOTOR USING NEURAL NETWORK” is the result of my own research except as cited in the references. The thesis has not been accepted for any degree and is not concurrently submitted in candidature of any other degree.

Signature :
Name : MOHD SHUKRI BIN ALIAS
Date : 29 NOVEMBER 2010

To my beloved mother and father and those who have guided and inspired me
throughout my journey of learning.

“I hereby acknowledge that the scope and quality of this thesis is qualified for the award of the Bachelor Degree of Electrical Engineering (Electronics)”

Signature : _____

Name : NORAZILA BT JAALAM

Date : 29 NOVEMBER 2010

ACKNOWLEDGEMENT

First of all, praise to God the most gracious and merciful that I have been able to finished this final year project (PSM) in the mean time.

During this project, I have received contribution and support from many people. In particular, I would like to express my thanks to my supervisor Pn Azila binti Jaalam for her ideas, encouragement, guidance and her kindness to me in order to do this project.

I also would like to thanks my father, Sir Alias Bin Yaacob and my mother, Madam Norhayati Binti Abdul Kadir because of their continuous morale support, encouragement and love had given me strength to finish up this course as well as this project. The same thank also to my siblings for their constructive ideas. Life would be meaningless without my family.

Last but not least, I would like to dedicate my appreciation to all my friends who assisted me upon my request and were very helpful with their ideas.

ABSTRACT

During the operation of induction motor, stator resistance changes incessantly with the temperature of the working machine. This situation may cause an error in rotor resistance estimation of the same magnitude and will produce an error between the actual and estimated motor torque which can leads to motor breakdown in worst cases. Therefore, this project will propose an approach to estimate stator resistance of induction motor using neural network. Then, a correction will be made to ensure the stabilization of the system.

This work has been motivated by the recent use of neural networks in different industry applications, and by their several advantages over the conventional controllers, such as stability, reliability, speed, and robustness.

ABSTRAK

Selama operasi motor induksi, perubahan rintangan stator berkadar terus dengan suhu mesin beroperasi . Situasi ini boleh menyebabkan kesalahan dalam anggaran ketahanan dengan nilai parameter yg sama dan akan menghasilkan kesalahan antara tujahan motor sebenar dan motor anggaran yang boleh menyebabkan kerosakan yang teruk pada motor. Oleh kerana itu, projek ini akan mencadangkan suatu pendekatan untuk memprediksi ketahanan stator motor induksi menggunakan rangkaian saraf tiruan. Kemudian, pembetulan akan dilakukan untuk memastikan kestabilan sistem.

Operasi ini telah didorong oleh penggunaan rangkaian saraf dalam aplikasi industri yang berbeza dengan beberapa kelebihan dalam pengawalan konvensional, seperti kestabilan, kebolehpercayaan, kelajuan, dan ketahanan.

TABLE OF CONTENTS

CHAPTER	TITLE	PAGE
	DECLARATION	ii
	DEDICATION	iii
	ACKNOWLEDGEMENT	iv
	ABSTRACT	v
	ABSTRAK	vi
	TABLE OF CONTENTS	vii
	LIST OF TABLES	ix
	LIST OF FIGURES	x
	LIST OF APPENDICES	xiii
	LIST OF SYMBOLS	xiv
	LIST OF ABBREVIATIONS	xv

TABLE OF CONTENTS

I	INTRODUCTION	
	1.0 Background	1
	1.1 Problem statement	2
	1.2 Objectives of the Project	2
	1.3 Scope of the project	2
	1.4 Thesis Outline	3
II	LITERATURE REVIEW	
	2.1 Introduction	4
	2.2 Condition monitoring	4
	2.3 Induction motor fault	5
	2.3.1 Voltage Drop	6
	2.3.2 Stator Winding Fault	6
	2.4 Artificial Intelligent	7
	2.4.1 Fuzzy Neural Network	8
	2.4.2 Genetic algorithms	9
	2.4.3 Parallel MRAS	10
III	METHODOLOGY	
	3.1 Chapter overview	12

3.2.0	Estimated Induction Motor	13
3.2.1	D-Axis Flux Rotor Model	14
3.2.2	Q-Axis Flux Rotor Model	15
3.2.3	D-Axis Stator Current	15
3.2.4	Q-Axis Stator Current	16
3.3	Actual Induction Motor	17
3.3.1	No Load	17
3.3.2	On Load	21
3.4	Neural Network Estimator	26
3.4.1	Generating the Training Data	26
3.4.2	Creating and Training the Neural Network	29
3.4.3	Testing the Trained Neural Network	30
3.5	Neural Network Correction	31
3.5.1	Development of NN Correction	32

IV RESULT & DISCUSSION

4.0	Introduction	34
4.1	No Load Analysis	34
4.2	On Load Analysis	36
4.3	Stator Resistance Estimation Analysis	38
4.4	Stator Resistance Correction Analysis	40

V CONCLUSION & RECOMMENDATION

5.0	Conclusion	41
5.1	Future Recommendation	42

LIST OF TABLES

TABLE NO	TITLE	PAGE
3.1	Rate Data of the Simulated Induction Motor at No Load	17
3.2	Rate Data of the Simulated Induction Motor at On Load	21

LIST OF FIGURES

FIGURE NO.	TITLE	PAGE
2.1	Types of induction machine faults.	7
2.2	The MRAS speed observer	12
3.1	Flow of the project	13
3.2	Estimated Induction Motor	13
3.3	Subsystem Estimated Induction Motor	14
3.4	Subsystem D-axis flux rotor	14
3.5	Subsystem Q-axis flux rotor	15
3.6	Subsystem D-axis stator current	15
3.7	Unmasked Q-axis stator current	16
3.8	Masked No Load Actual Induction Motor	17
3.9	No Load Actual Induction Motor Modeling in NUDSL	18
3.10	Three Phase supply	19
3.11	DQ to 3PH	19
3.12	DQ to Three Phase Block	19

3.13	3PH to DQ	20
3.14	Three Phases to DQ Block	20
3.15	Voltage Fed	20
3.16	Voltage Fed Induction Motor Block	21
3.17	Masked On Load Induction Motor	21
3.18	Subsystem Actual Induction Motor Block	22
3.19	Three Phase supply	23
3.20	DQ to 3PH	23
3.21	DQ to Three Phase Block	23
3.22	3PH to DQ	24
3.23	Three Phases to DQ Block	24
3.24	Voltage Fed	24
3.25	Voltage Fed Induction Motor Block	25
3.26	Mechanical Dynamic	25
3.27	Subsystem Mechanical Dynamic Block	25
3.28	Simulink model used to generate the training data	27
3.29	Simulation parameters configuration	27
3.30	Input block parameters	28
3.31	Input/output training pattern	29
3.32	Generating simulink model of ANN Estimator	30
3.33	Simulink model of NN model testing	30
3.34	Actual plant and NN model outputs	31
3.35	Correction simulink block	32
3.36	Input block parameter	33
3.37	Simulink model of ANN Estimator	33

4.1	Stator Current $I_s(k)$ at no load	34
4.2	Torque at no load	35
4.3	Speed of rotor at no load	36
4.4	Stator Current $I_s(k)$ at on load	36
4.5	Torque at on load	37
4.6	Speed of rotor at on load	37
4.7	Current error between actual and estimated induction motor	38
4.8	Change of stator resistance (ΔR_s).	39
4.9	Stator resistance estimation using ANN	39
4.10	Stator resistance correction using ANN	40

LIST OF APPENDICES

APPENDIX	TITLE
A	Mathematical Expressions for Estimated Induction Motor
B	ANN Estimator
C	ANN Correction
D	Block Diagram of Stator Resistance Estimation of Induction Motor

LIST OF SYMBOLS

V_{ds}	-	<i>Direct</i> component of the stator voltage vector
V_{qs}	-	<i>quadrature</i> component of the stator voltage vector
I_{ds}	-	<i>Direct</i> component of the stator current vector
I_{qs}	-	<i>quadrature</i> component of the stator current vector
λ_{ds}	-	<i>Direct</i> component of the rotor flux vector
λ_{qs}	-	<i>quadrature</i> component of the rotor flux vector
L_s	-	Stator inductance
L_r	-	Rotor inductance
L_m	-	Mutual inductance
R_s	-	Resistance of a stator phase winding
R_r	-	Resistance of a rotor phase winding
T_s	-	Stator time constant
T_r	-	Rotor time constant
σ	-	$1 - \frac{L_m^2}{(L_s L_r)}$ total leakage factor
ω_r	-	Rotor electrical angular velocity

LIST OF ABBREVIATIONS

ANN	Artificial Neural Network
(Δi_s)	Change Current Stator
R_s	Stator Resistance
(ΔR_s) .	Stator Resistance Change
BP	Back-Propagation
ZOH	Zero Order Hold

Chapter I

INTRODUCTION

1.0 Background

For induction motor drives controlled by the indirect rotor flux oriented control (IRFOC), the rotor resistance variation results in an undesirable coupling between the flux and the torque of the machine, and loss of dynamic performance. This paper presents a scheme for the estimation of rotor resistance using a neural networks (NN) block. In this system the flux and torque have been estimated by using stator voltages and currents. A back-propagation NN receives the flux and torque errors and a supposed rotor resistance at the input and estimates the actual rotor resistance at the output, which is used in the control of an indirect vector-controlled drive system.

The neural network has been trained off line with the mathematical model of the control scheme in detuning operations. IRFOC control, used with the NN estimator, has been studied in the detuning condition. The performance of the controller is good, even when the rotor time constant is increased from nominal rate to twice the nominal value, as well as torque variations. In this method, estimation is done quickly and accurately, and its design is simple.

Correction for the resistance value will make during the detuning process. The induction motor will operate at normal condition when the process finish.

1.1 Problem statement

The increased in demand has greatly improved the approach of fault detection in induction motor. During the operation of induction motor, stator resistance changes incessantly with the temperature of the working machine. This situation may cause an error in rotor resistance estimation of the same magnitude and will produce an error between the actual and estimated motor torque which can leads to motor breakdown in worst cases. Nowadays artificial intelligence is implemented to improve traditional techniques, where the results can be obtained instantaneously after it analyzes the input data of the motor.

1.2 Objectives of the project

The main objective of this project is to estimate the changes of induction motor stator resistance using neural network from the simulation result that is use to make a correction to ensure the stabilization of the system. This simulation can make motor run smooth and easier to make correction for the real application.

1.3 Scope of the project

This project will focus on construction the induction motor, estimation the stator resistance using neural network and make the correction from the data that have been taken. However this project is using software only and application for the real motor are out of this project. The function of neural network is estimate the R_s value only not controlling or to make another function. The correction then will be made by using the Neural Network software to ensure the stabilization of the system.

1.4 Thesis outline

This thesis consists of five chapters. In the first chapter, this chapter discussed the overall idea of this project including background, objectives of project, the scope of this project and summary of this thesis.

Chapter 2 discussed more on theory and literature review that have been done. It is well discusses about the Artificial Intelligence (AI), basic concept of the fault in induction motor related to this project.

Chapter 3 described briefly the methodology of the estimated induction motor, neural network estimator and develops correction for this project. This part also includes flow chart, and circuit design of the system.

Chapter 4 presents a discussion of the implementation, result and analysis of the whole project.

Chapter 5 provides the conclusions of the project. There are also several suggestions that can be used for future implementation or recommendation for this project.

CHAPTER II

LITERATURE REVIEW

2.1 Introduction

This chapter includes all the paper works and related research as well as the studies regards to this project. The chapter includes all important studies which have been done previously by other research work. The related works have been referred carefully since some of the knowledge and suggestions from the previous work can be implemented for this project.

Literature review was an ongoing process throughout the whole process of the project. It is very essential to refer to the variety of sources in order to gain more knowledge and skills to complete this project. These sources include reference books, thesis, journals and also the materials obtained from internet.

At the beginning of the project, the basic concept of fault in induction motor has been well acquired. In addition, the function of all the components used in this project such as basic operation of MATLAB, Neural Network variations, and so on was explored first before starting the project.

2.2 Condition Monitoring

During the past twenty years, there has been a substantial amount of research into the creation of new condition monitoring techniques for electrical machine drives, with new methods being developed and implemented in commercial products for this purpose [1]. On-line condition monitoring involves taking measurements on

a machine while it is operating in order to detect faults with the aim of reducing both unexpected failures and maintenance costs. Artificial intelligence is used because of its abilities to do analysis where formal analysis would be difficult or impossible, such as pattern recognition and nonlinear system identification and control. [2]

2.3 Induction Motor Fault

Induction motors play an important role in manufacturing environments, therefore, this type of machine is mainly considered and many diagnostic procedures are proposed both from industry and from academia [3].

A fault in a component is usually defined as a condition of reduced capability related to specified minimal requirements and is the result of normal wear, poor specification or design, poor mounting (here also including poor alignment), wrong use, or a combination of these. If a fault is not detected or if it is allowed to develop further it may lead to a failure [4].

The major faults of electrical machines can broadly be classified as the following [3]:

- Stator faults resulting in the opening or shorting of one or more of a stator phase winding.
- Abnormal connection of the stator windings.
- Broken rotor bar or cracked rotor end-rings.
- Static and/or dynamic air-gap irregularities.
- Shorted rotor field winding.
- Bearing and gearbox failures.

Induction machine failure surveys have found the most common failure mechanisms in induction machines [5]. These have been categorized according to the main components of a machine—stator related faults, rotor related faults, bearing related faults and other faults.

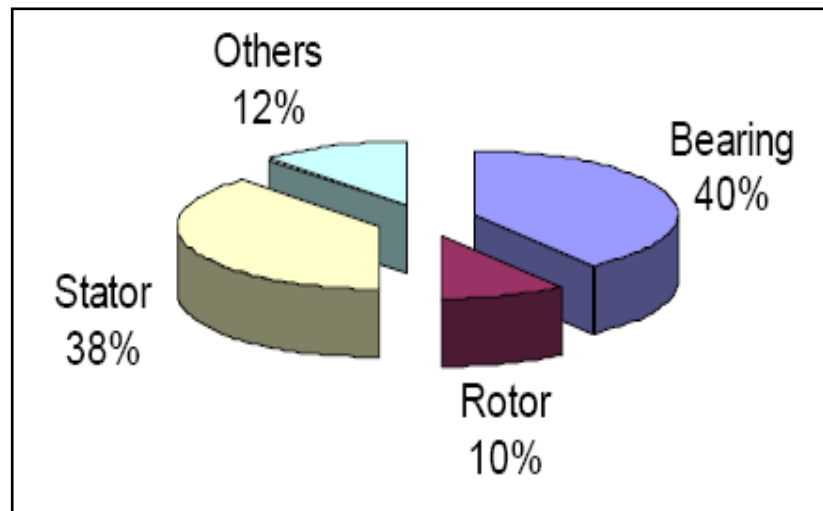


Figure 2.1: Types of induction machine faults.

2.3.1 Voltage Drop

When line voltages applied to a uniphase induction motor are not exactly the same. The effect on the motor can be severe and the motor may overheat to the point of burnout. The voltages should be as closely as can be read on the usually available commercial voltmeter.

2.3.2 Stator Winding Fault

Almost 40% of all reported induction machine failures fall into this category. The stator winding consists of coils of insulated copper wire placed in the stator slots.

Stator winding faults are often caused by insulation failure between two adjacent turns in a coil. This is called a turn-to-turn fault or shorted turn. The resultant induced currents produce extra heating and cause an imbalance in the magnetic field in the machine. If undetected, the local heating will cause further damage to the stator insulation until catastrophic failure occurs. The unbalanced magnetic field can also result in excessive vibration that can cause premature bearing failures [6].

Some of the most frequent causes of stator winding failures are [5]:

- High stator core or winding temperatures.
- Slack core lamination, slot wedges, and joints.
- Loose bracing for end winding.
- Contamination caused by oil, moisture, and dirt.
- Short circuits.
- Starting stresses.
- Electrical discharges.

2.4 Artificial Intelligence

The essence of an expert system is the ability to manage knowledge-based production rules that model the physical system, while it is a main feature of NNs that they are general nonlinear function approximators. This function approximation is achieved by using an appropriate network built up from artificial neurons, which are connected by appropriate weights. However, the exact architecture of a NN is not known in advance; it is usually obtained after a trial and error procedure. Fuzzy logic systems are expert, rule-based systems, but they can also be considered to be general nonlinear function approximators. In contrast to NNs, they give a very clear physical description of how the function approximation is performed (since the rules show clearly the function approximation mechanism). On the other hand, fuzzy-NNs are basically NNs with fuzzy features, and it is one main advantage over “pure” NNs that their architecture is well defined [7]. Research trends show that AI techniques will have a greater role in electrical motor diagnostic system with advance practicability, sensitivity, reliability and automation. Diagnostic system based upon fuzzy neural will be very extensively used. Self-repairing electrical drives based upon genetic-algorithm-assisted neural and fuzzy neural systems will also be widely used in the near future [8], [9]. The explored opportunities are to add intelligence to motors, providing a level of communication and diagnostic capability [2], [10].

2.4.1 Fuzzy Neural Network

Direct torque control (DTC) system has been extensively applied to the induction motor drive because of its advantages that has good static and dynamic performance. The control method takes torque and flux linkage as control object in stator coordinate. It removes complicated coordinate transformation and cannot be influenced by rotor parameters. In DTC system, the stator resistance mainly influences observation of the stator flux linkage and torque. At high speed, the error of the flux linkage caused by stator resistance can be ignored. However, at low speed, the voltage drop caused by stator resistance current cannot be ignored.

Accordingly, the accurate observation of stator resistance is the key to improving system performance at low speed. [11]and[12] give two fuzzy resistance estimators that can carry out on-line estimation of the stator resistance. Because it is influenced by artificial factors to select membership functions of input linguistic variable and establish control rules. If the selection is improper, experiment results will not satisfactory, even system performance will be completely destroyed. In [13]and[14], the stator resistance estimator is composed of a three-layer BP neural network, but the neural net needs long training time and falls easily into local minimum. In the paper, a fuzzy-neural network (FNN) can optimize membership function and fuzzy rule by making use of its self-organizing learning. In this way, the deficiencies that exist in fuzzy resistance estimators and neural network resistance estimators will be made up. The performance at low speed of DTC system is efficiently improved.

2.4.2 Parameter Identification using GA (Genetic Algorithm)

For parameter identification of induction motor, we used mathematical model of motor in stator coordinate system described in [15]. For this model we need to identify the values of stator and rotor resistance, stator and rotor inductance, magnetizing inductance and moment of inertia. The two parameters L_s and L_r are linearly dependent [16] and the differences between their values are small. Therefore we used simplification $L_r = L_s$, and so reduced the number of the searched parameters and thereby accelerated the research process. Searched motor parameters represent genes of GA and together create the chromosome, which has a form:

$$r = (R_s, R_r, L_s, L_m, J)$$

To represent these parameters we choose real number values. In using real number code in comparison with binary code the procedure of the respective solution is more stable, since the values of real numbers change continuously, proportionally to the required value of change. For each gene of the chromosome we must define the feasible values intervals, i.e. the search space of solution. The search space must be large enough to contain the global optimum, but if made too large, the GA might not be able to find the global optimum at the required parameter identification accuracy and in a reasonable period of time (the convergence will be slow). For this, we can start from catalogue values. The speed of convergence is also influenced by our choice of the population size. The population represents group of chromosomes, i.e. potential solutions in the time period. The size of it depends on a particular case. In most cases it is recommended to choose the size between 10 and 100, most frequently between 20 and 50[17].

Small population does not provide enough space for diversity of genetic information, too big population does not provide better effect and the solution is much longer. The GA tests each candidate – chromosome by an objective function, which compare a set of measured values with simulated data. The objective function consists of two steps. The first one is the implementation of parameters into simulation model and the following simulation of the dynamic system with such input data as for measured system. During the simulation, the system output is

recorded in each sampling period and this output data are then returned into the quality criterion with measured output data. The next step is the calculation of the appropriate criterion. The identification values of the system parameters approximate to their real values by the minimalization of this criterion. For the parameter identification, the integral criterion is used:

$$F = \int_0^T (y - y_m)^2 dt$$

Where, y_m is output of the simulation model and y is output of the real system.

2.4.3 Parallel MRAS Estimation of Rotor Speed and Stator Resistance

The system block diagram of a conventional MRAS speed observer is shown in Figure 2 and includes a reference model (1), an adjustable model (2), and an adaptive ω mechanism (3). Both models are excited by measured stator voltages and/or currents. The reference model specifies a given rotor flux ψ_{rv}^s . The difference of phase angle between outputs of these two models is used by the adaptive mechanism to converge the estimated ω to its true value. The second piece of information of the vector product (3) is unused. Therefore, in order to allow the continuous tracking of non-predictable thermal R_s changes, there is a basis for using ψ_{rv}^s and ψ_{rv}^s in added adaptation mechanisms (Figure 1b). The adaptation mechanism for the on-line tuning of R_s (4), proposed in this letter, is derived by hyper stability theory [18].

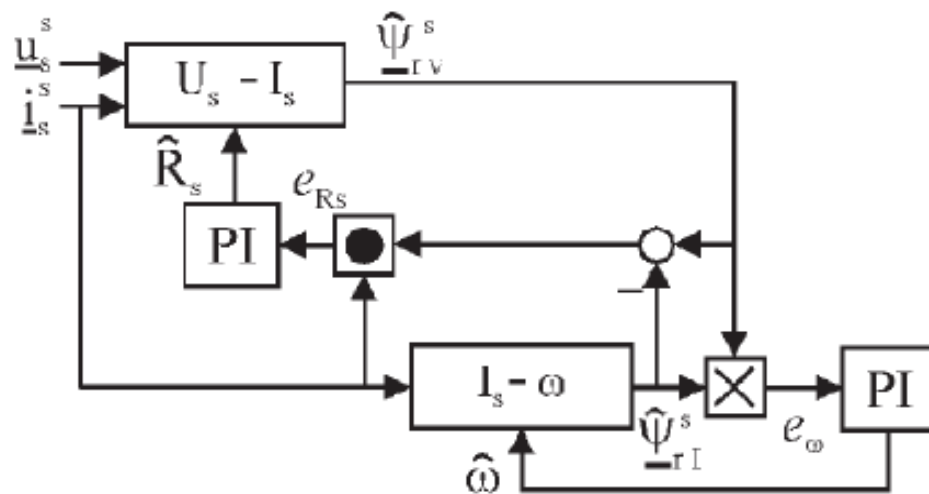
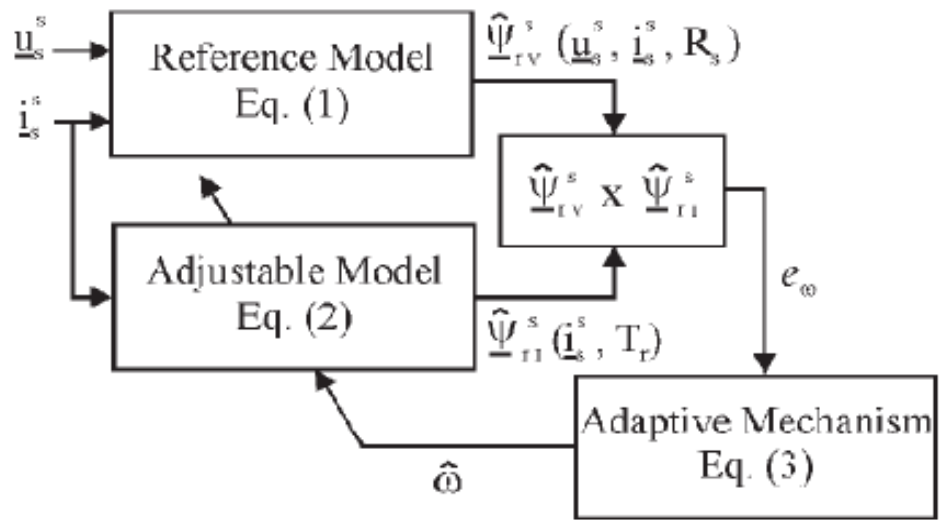


Figure 2.2: The MRAS speed observer; (a) the basic configuration, (b) configuration for parallel rotor speed and stator resistance estimation.

CHAPTER III

METHODOLOGY

3.1 Chapter Overview

This chapter will explain about the method that has been done to complete the project. Basically, the project will be divided into few parts and the project will be executed stage by stage. After the title has been decided, the first thing to do is to have a clear understanding about the whole idea of the project.

This chapter divided to two main parts. First is developing induction motor by using equation. The equation was written in the Matlab simulink block. Then the Neural Network will be developing by using Matlab simulink and the program will be written in the M-file. The whole system of the project can be overview by flow chart is shown in Figure 3.1.

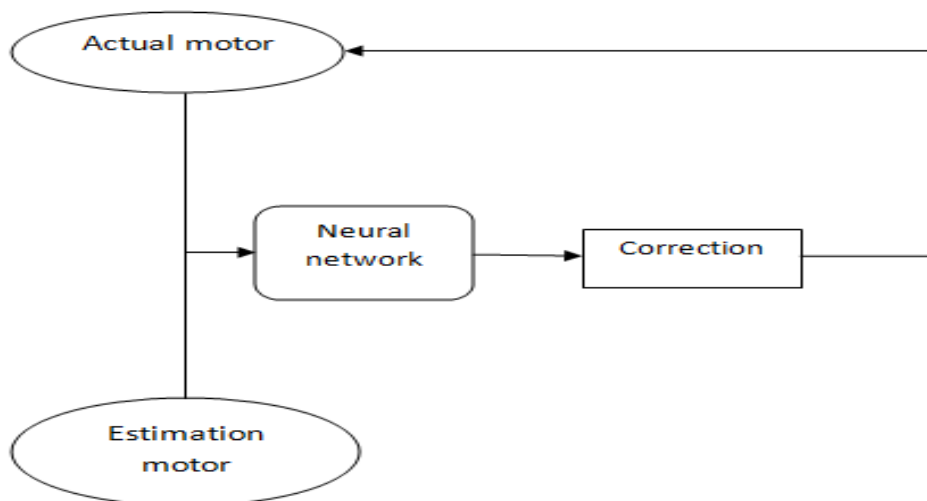


Figure 3.1: Flow of the project.

3.2 Estimated Induction Motor

In this method, by referring the equation from IEEE library, the estimated induction motor was designed. There are two equations involved which are based on stator voltages and stator currents and another one is stator currents and rotor speed.

This induction motor was designed refer to dq frame model. The choice of the common dq frame is usually dictated by the symmetry constraints imposed by the construction and excitation of the machine. Then the sub-subsystem will be creating like shown in figure 3.2. In the block have 4 main subsystems such as shown in the figure 3.3.

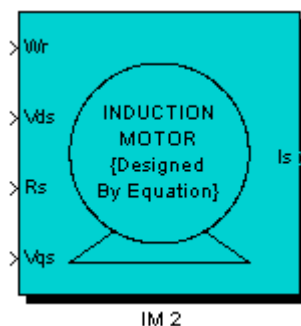


Figure 3.2: Estimated Induction Motor

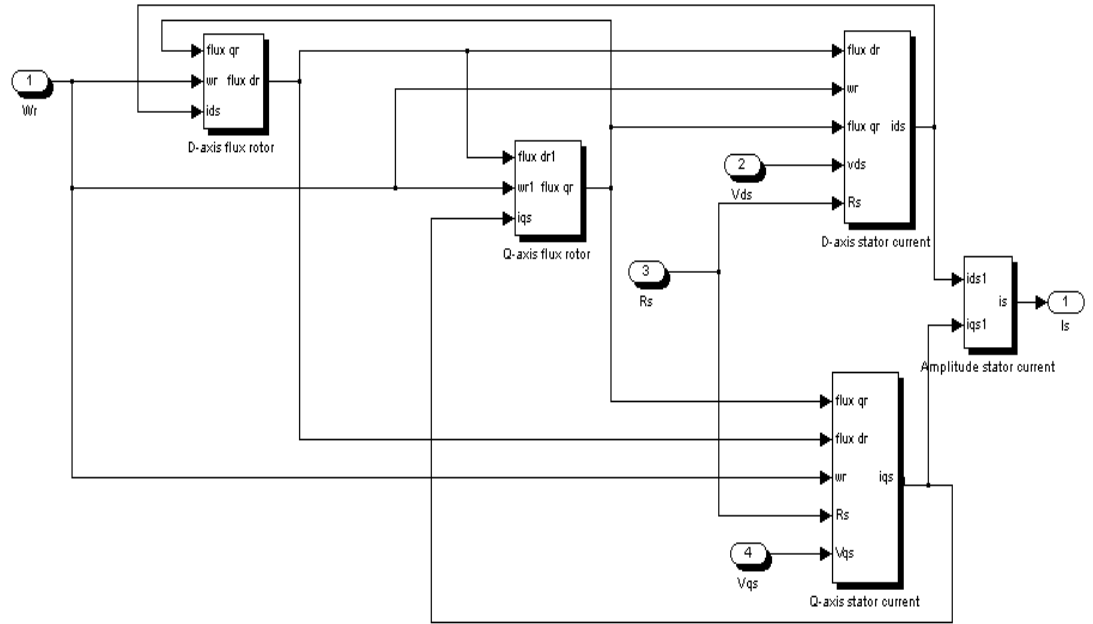


Figure 3.3: Subsystem Estimated Induction Motor

3.2.1 D-Axis Flux Rotor Model

The block model was designed based on stator currents and rotor speed equation matrix. Figure 3.4 below shows a D-axis flux rotor model which has been developed by using equation (1).

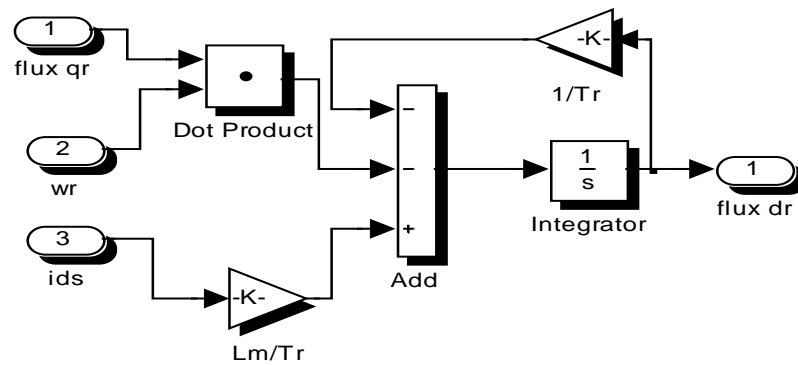


Figure 3.4: Subsystem D-axis flux rotor

$$\frac{d\lambda_{dr}^{sim}}{dt} = -\frac{1}{T_r} \lambda_{dr}^{sim} - \omega_r \lambda_{qr}^{sim} + \frac{L_m}{T_r} i_{ds}^s \quad (1)$$

3.2.2 Q-Axis Flux Rotor Model

The block showed in the figure 3.5 below shows the equation of Q-axis flux rotor model refer to equation (2). The block model was designed using stator currents and rotor speed equation matrix.

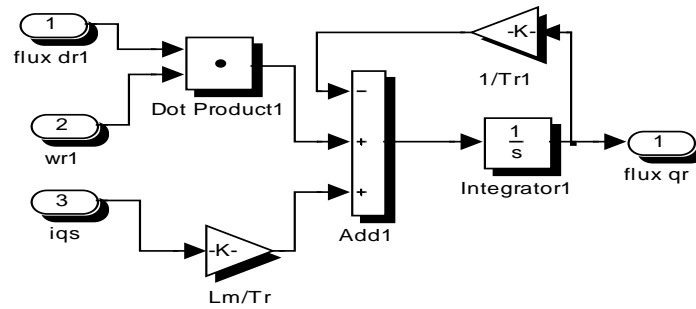


Figure 3.5: Subsystem Q-axis flux rotor

$$\frac{d\lambda_{qr}^{s\,im}}{dt} = \omega_r \lambda_{dr}^{s\,im} - \frac{1}{T_r} \lambda_{qr}^{s\,im} + \frac{L_m}{T_r} i_{qs}^s \quad (2)$$

3.2.3 D-Axis Stator Current

The figure 3.6 shows the equation of D-axis stator current model written in simulink block using equation (3).

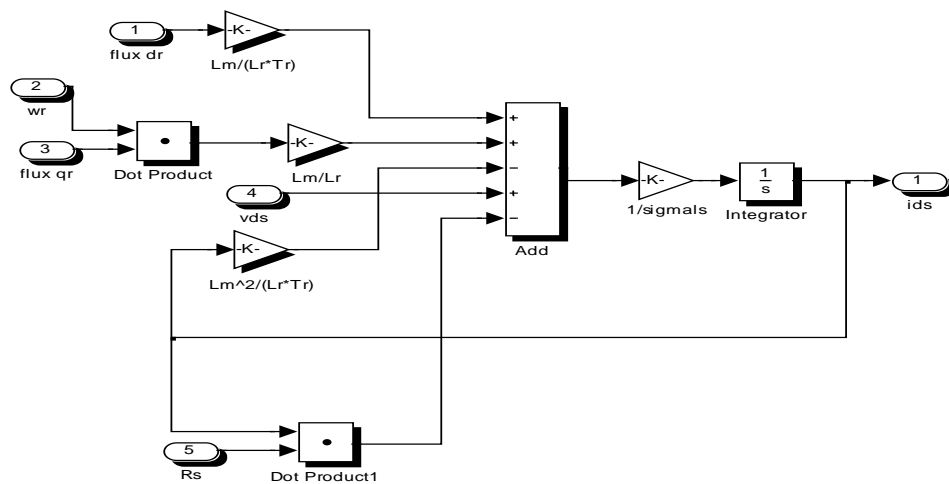


Figure 3.6: Subsystem D-axis stator current

$$\sigma L_s \frac{di_{ds}^s}{dt} = \frac{L_m}{L_r T_r} \lambda^{s im}_{dr} + \frac{L_m}{L_r} \omega \lambda^{s im}_{qr} - \frac{L_m^2}{L_r T_r} i_{ds}^s + v_{ds}^s - R_s i_{ds}^s \quad (3)$$

3.2.4 Q-Axis Stator Current

The figure 3.7 shows the equation of D-axis stator current model written in simulink block using equation (4).

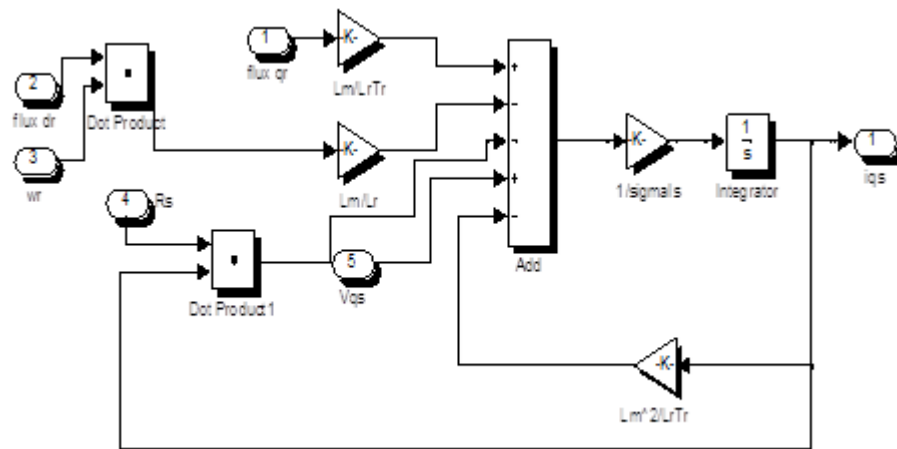


Figure 3.7: Unmasked Q-axis stator current

$$\sigma L_s \frac{di_{qs}^s}{dt} = \frac{L_m}{L_r T_r} \lambda^{sim}_{qr} - \frac{L_m}{L_r} \omega \lambda^{sim}_{dr} - \frac{L_m^2}{L_r T_r} i_{qs}^s + v_{qs}^s - R_s i_{qs}^s \quad (4)$$

3.3 Actual Induction Motor

For actual induction motor, it focuses on Newcastle University Drive Simulink Library (N.U.D.S.L). Actual induction is simulated using Simulink block from this library. Here, there are two conditions should be considered in designing induction motor, which are no load and on load conditions.

3.3.1 No Load

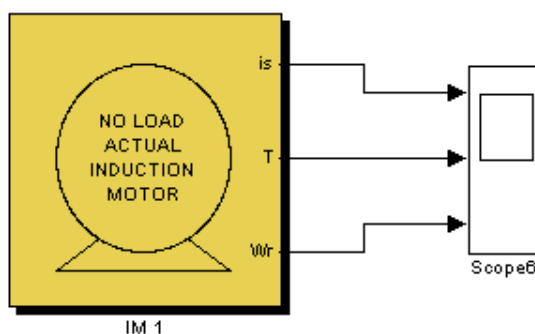


Figure 3.8: Masked No Load Actual Induction Motor

Figure 3.8 shows the simulink block induction motor that was design using Newcastle University Drive Simulink Library (N.U.D.S.L). The parameter value can be referring in Table 3.1.

Table 3.1 Rate Data of the Simulated Induction Motor at No Load

Power	4kW
Frequency	50 Hz
Voltage	220/380
Current	15/8.6 A
Rpm	1440
Connection	Δ / Y
Power factor	0.8
Stator Resistance, R_s	1.2 Ω
Rotor Resistance, R_r	1.8 Ω
Stator Inductance, L_s	0.156 H
Rotor Inductance, L_r	0.156 H
Mutual Inductance, L_m	0.143 H

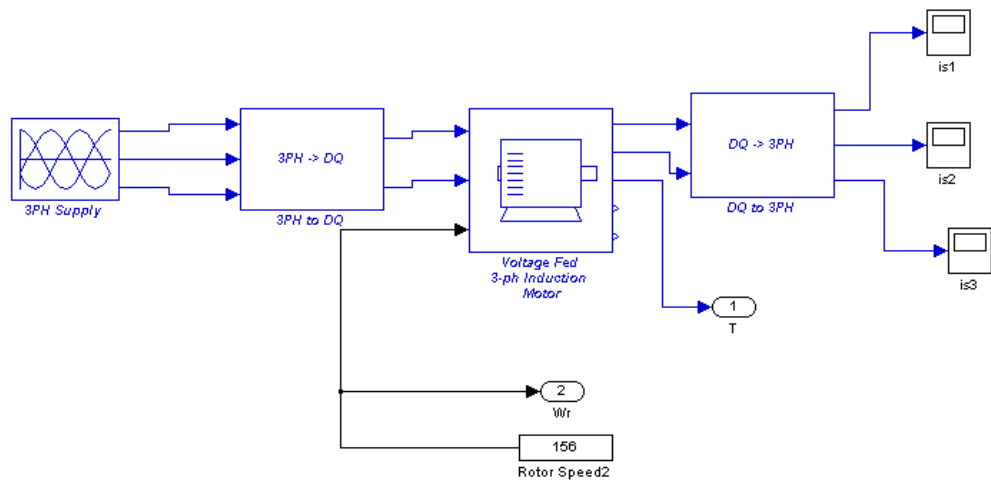


Figure 3.9: No Load Actual Induction Motor Modeling in NUDSL

Synchronous Speed

$$n_{sync} = \frac{120f_e}{P}$$

$$= \frac{120 \times 50}{2}$$

$$= 3000rpm$$

$$\omega_{sync} = 3000rpm \times \frac{2\pi \text{ rad}}{1r} \times \frac{1 \text{ min}}{60s}$$

$$= 314.1592 \text{ rad / s}$$

Rotor Speed

$$\omega_r = \frac{2\pi f}{P}$$

$$= \frac{2\pi \times 50}{2}$$

$$= 157.0796 \text{ rad / s}$$

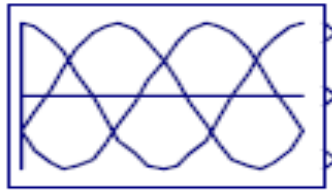


Figure 3.10: Three Phase supply

The three phase supply as shown in figure 3.10 has no inputs and three outputs which are 'A' Phase voltage, 'B' Phase voltage and 'C' Phase voltage.

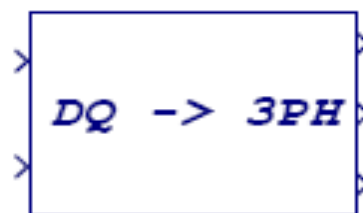


Figure 3.11: DQ to 3PH

The DQ to 3PH block as shown in figure 3.11 has two inputs, D-Axis Value, Q-Axis Value. Three outputs are Phase 'A' Value, Phase 'B' Value, and Phase 'C' Value. Figure 3.12 shows the subsystem for the DQ to 3PH block.

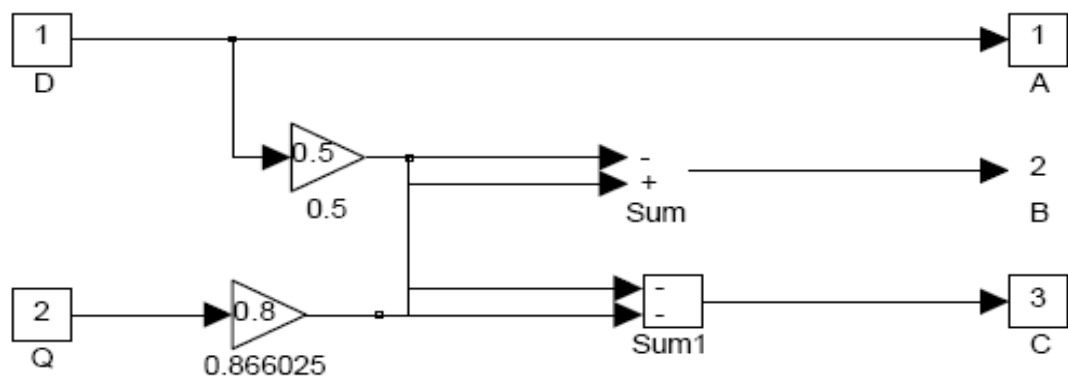


Figure 3.12: DQ to Three Phase Block



Figure 3.13: 3PH to DQ

The 3PH to DQ block in the figure 3.13 has three inputs which are Phase 'A' Value, Phase 'B' Value, Phase 'C' value. The outputs are D-Axis Value and Q-Axis Value. The subsystem for this block is shown in the figure 3.14.

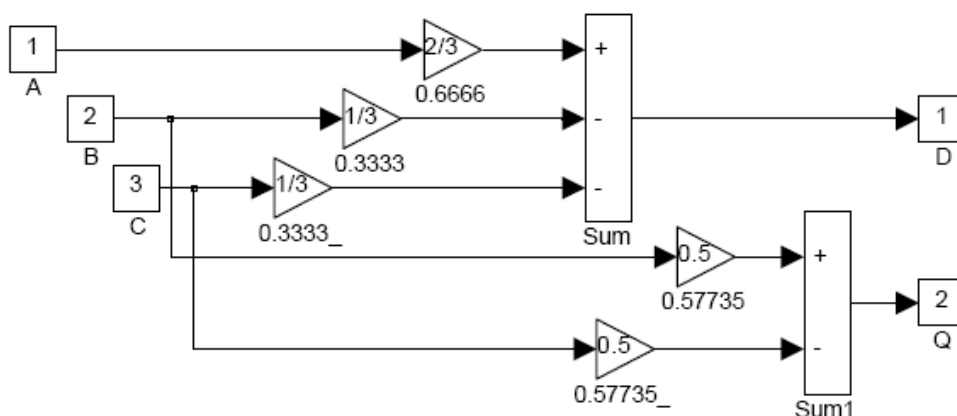


Figure 3.14: Three Phases to DQ Block

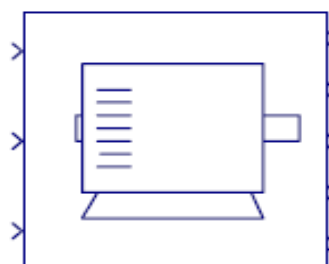


Figure 3.15: Voltage Fed

The Induction Motor Model block as shown in figure 3.15 has three inputs which are D-Axis Stator Voltage, Stator Voltage (stator ref. frame) and Rotor Speed (rads/sec). The outputs are D-Axis Stator Current (stator ref. frame), Q-Axis Stator Current (stator ref. frame), Electromagnetic Torque, D-Axis Rotor Current (stator ref. frame), and Q-Axis Rotor Current (stator ref. frame). The subsystem for this block is shown in the figure 3.16.

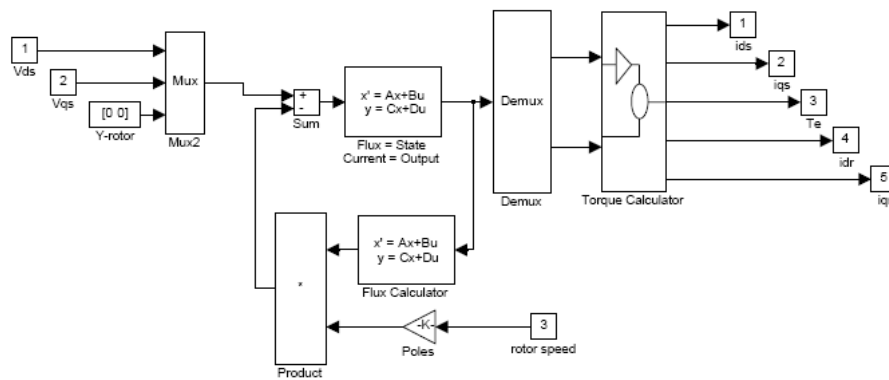


Figure 3.16: Voltage Fed Induction Motor Block

3.3.2 On Load

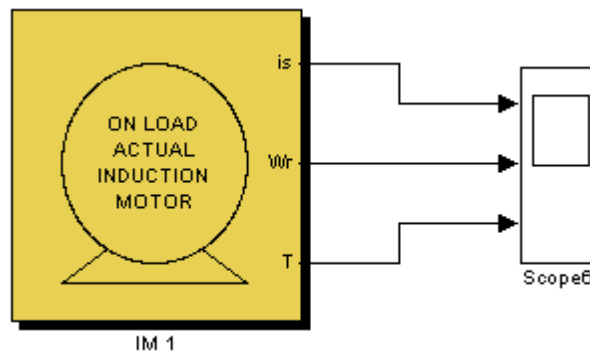


Figure 3.17: Masked On Load Induction Motor

Power	4kW
Frequency	50 Hz
Voltage	220/380
Current	15/8.6 A
Rpm	1440
Connection	Δ / Y
Power factor	0.8
Stator Resistance, Rs	1.2 Ω
Rotor Resistance, Rr	1.8 Ω
Stator Inductance, Ls	0.156 H
Rotor Inductance, Lr	0.156 H
Mutual Inductance, Lm	0.143 H
Moment Inertia, J	0.024 kgm ²

Table 3.2: Rate Data of the Simulated Induction Motor at On Load

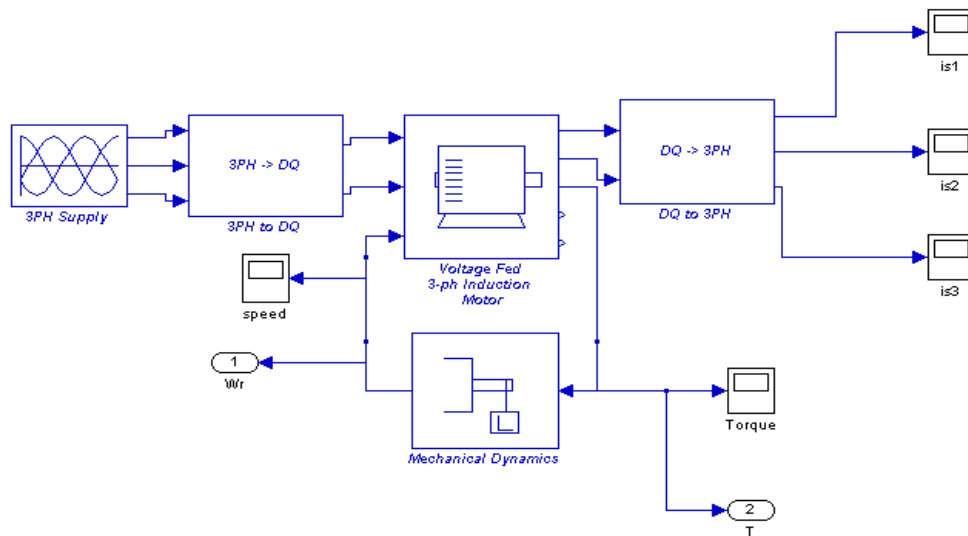


Figure 3.18: Subsystem Actual Induction Motor Block

From display block, $\omega_r = 151.6 \text{ rad/s}$

Synchronous speed, $\omega_{sync} = 314.1592 \text{ rad/s}$

$$\begin{aligned} Slip &= \frac{\omega_{sync} - \omega_r}{\omega_{sync}} \\ &= 0.5174 \end{aligned}$$

Torque rated

$$\begin{aligned} T_{rated} &= \frac{P_{out}}{\omega_r} \\ &= \frac{4000 \text{ W}}{151.6} = 26.385 \text{ Nm} \end{aligned}$$

Torque load

$$\begin{aligned} T_L &= \frac{80}{100} \times T_{rated} \\ &= \frac{80}{100} \times 26.525 \text{ Nm} \\ &= 21.108 \text{ Nm} \end{aligned}$$

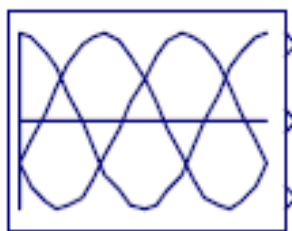


Figure 3.19: Three Phase supply

The three phase supply in figure 3.19 has no inputs and three outputs which are 'A' Phase voltage, 'B' Phase voltage and 'C' Phase voltage that function to supply input for induction motor.

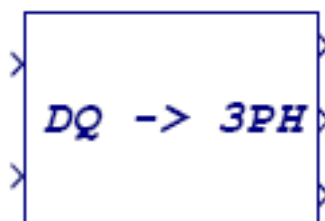


Figure 3.20: DQ to 3PH

The DQ to 3PH block in figure 3.20 has two inputs, D-Axis Value, Q-Axis value that convert from one phase to three phase output. Three outputs are Phase 'A' Value, Phase 'B' Value, and Phase 'C' Value. The subsystem for the DQ to 3PH block showed in the figure 3.21.

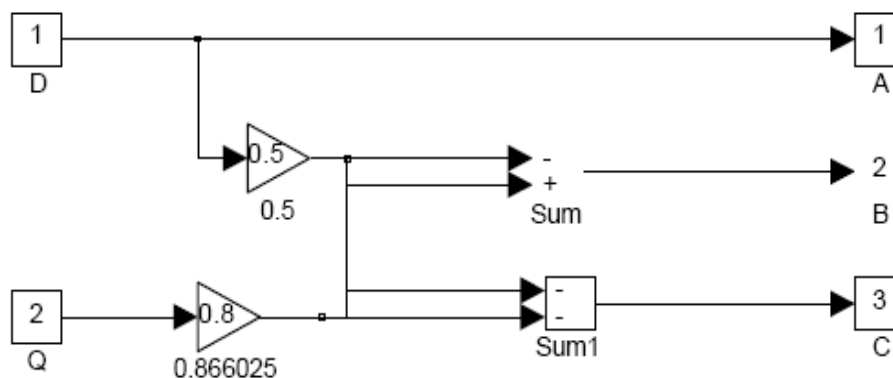


Figure 3.21: DQ to Three Phase Block

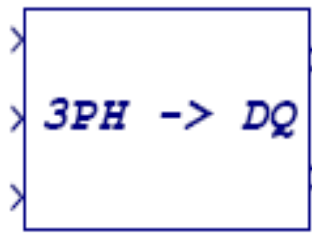


Figure 3.22: 3PH to DQ

The 3PH to DQ block figure 3.22 has three inputs which are Phase 'A' Value, Phase 'B' Value, Phase 'C' value that convert to one phase output. The outputs are D-Axis Value, Q-Axis value that their subsystem shown in the figure 3.23.

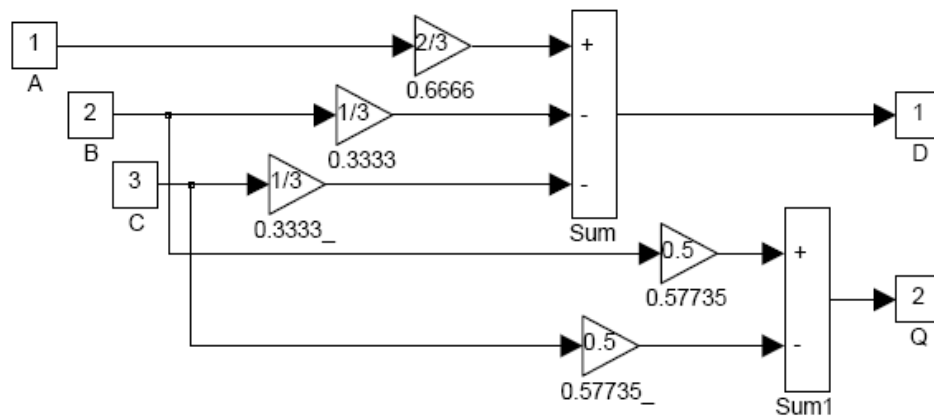


Figure 3.23: Three Phases to DQ Block

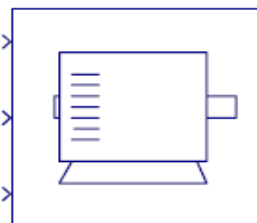


Figure 3.24: Voltage Fed

The Induction Motor Model block in figure 3.24 has three inputs which are D-Axis Stator Voltage, Q-Axis Stator Voltage (stator ref. frame) and Rotor Speed (rads/sec). The outputs are D-Axis Stator Current (stator ref. frame), Q-Axis Stator

Current (stator ref. frame), Electromagnetic Torque, D-Axis Rotor Current (stator ref. frame), and Q-Axis Rotor Current (stator ref. frame). The construction of this block below is showed in figure 3.25.

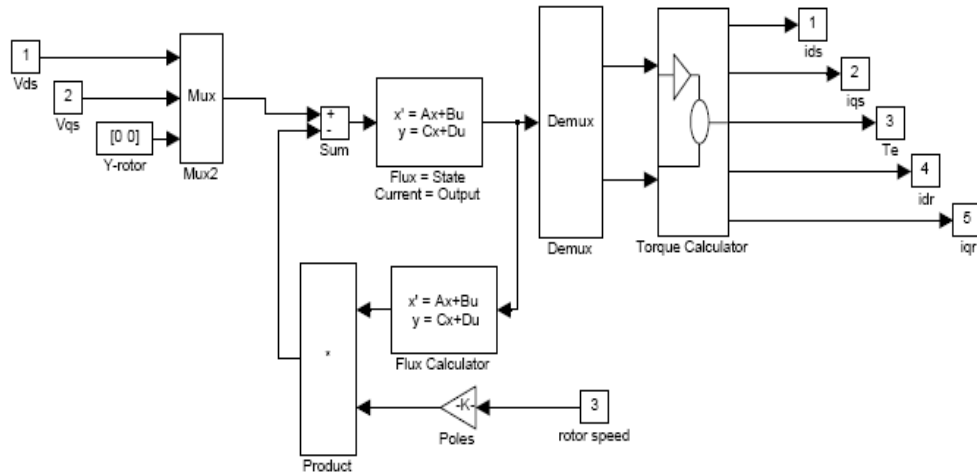


Figure 3.25: Voltage Fed Induction Motor Block

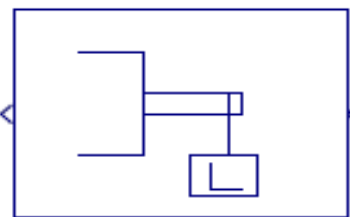


Figure 3.26: Mechanical Dynamic

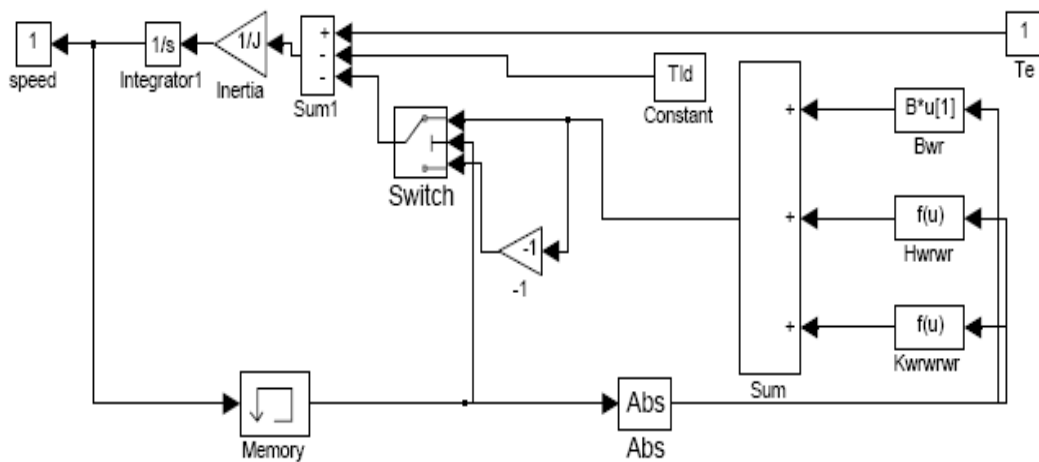


Figure 3.27: Subsystem Mechanical Dynamic Block

Figure 3.26 shows the Mechanical Dynamics and figure 3.27 shows its subsystem that have block one input, electromagnetic Torque and one output, rotor Speed (rads/sec).

3.4 Neural Network Estimator

Neural network estimator designed using simulink block and M-file in MATLAB. Artificial Neural Network (ANN) have been powerfully applied in the field of automatic control in system identification, adaptive control, parameter estimation and optimization and a lot of other applications in this field.

In this application, the plant model is not available. Neural networks can be trained to learn the unknown model of the plant using input/output data obtain experimentally from the plant.

3.4.1 Generating the Training Data

This will be done by subjecting the plant to a sequence of input p and obtaining the corresponding output t . The simulink model is shown in figure 3.28. The simulation parameters were adjusted as in figure 3.29 and the ZOH sampling time was adjusted to $1e-3$. The Band-limited white noise was chosen as the training input generates normally distributed random input. The power was adjusted to 0.1, sampling time to 0.1 and seed to 23341 as shown in figure 3.30. The block was used to workspace to save the training data in array format. The input was named p and the output was named to t . The simulation time was set to 10 and simulation was started. After the end of simulation, the workspace was looked at that figure should find the arrays representing p and t or open the scopes representing the input and output as shown in figure 3.31.

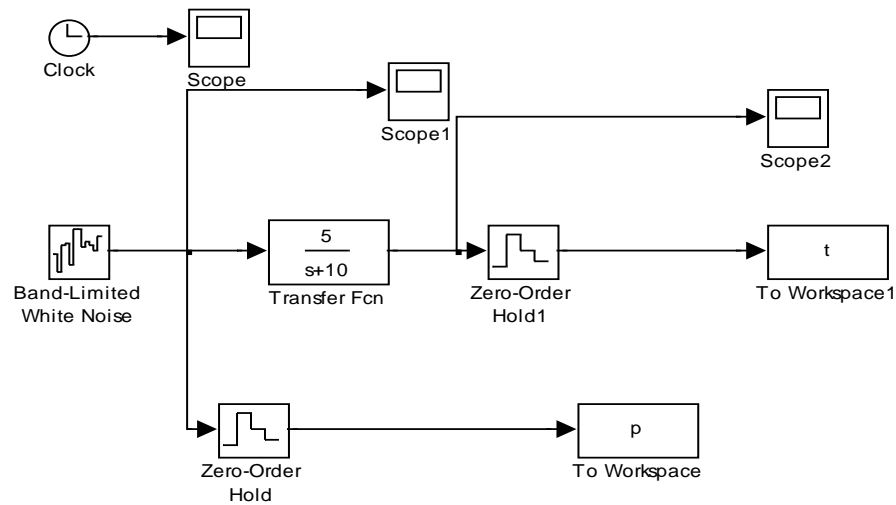


Figure 3.28: Simulink model used to generate the training data

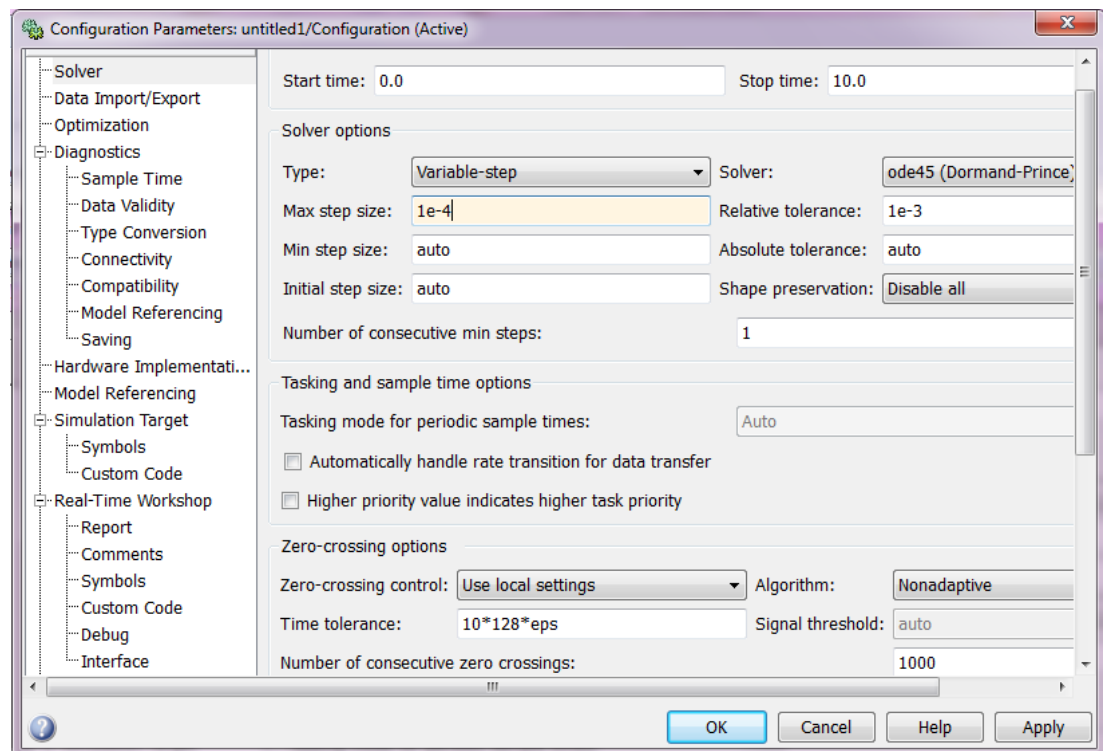


Figure 3.29: Simulation parameters configuration

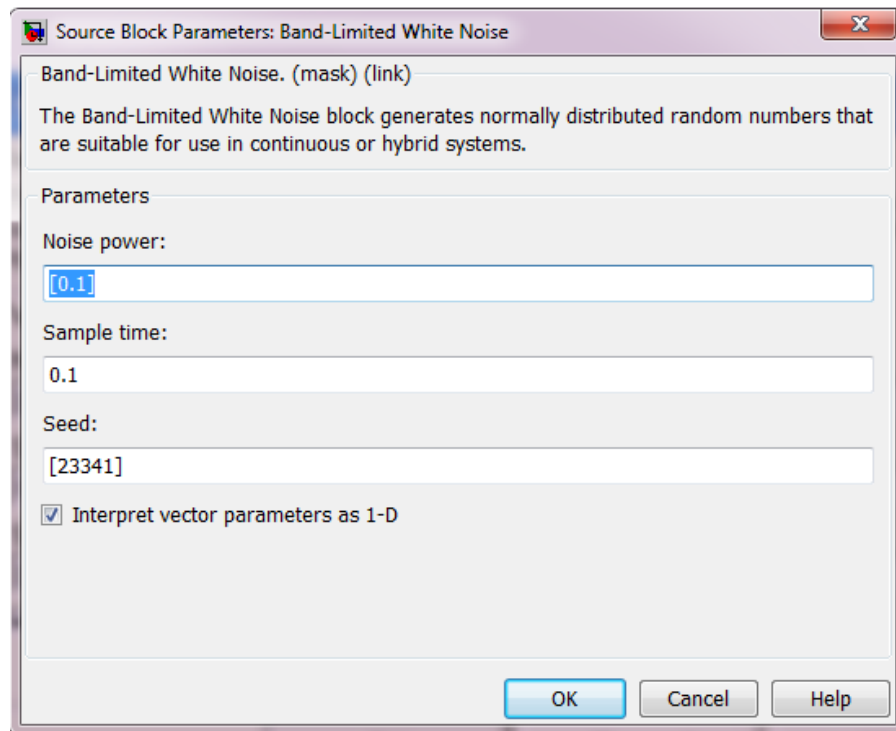
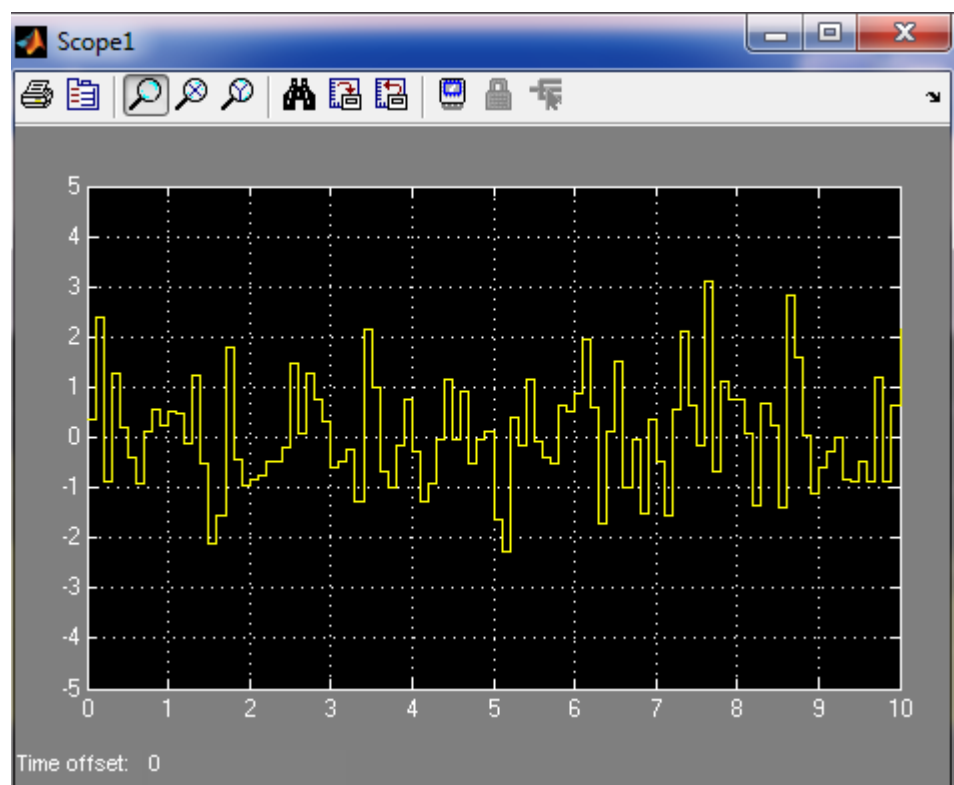
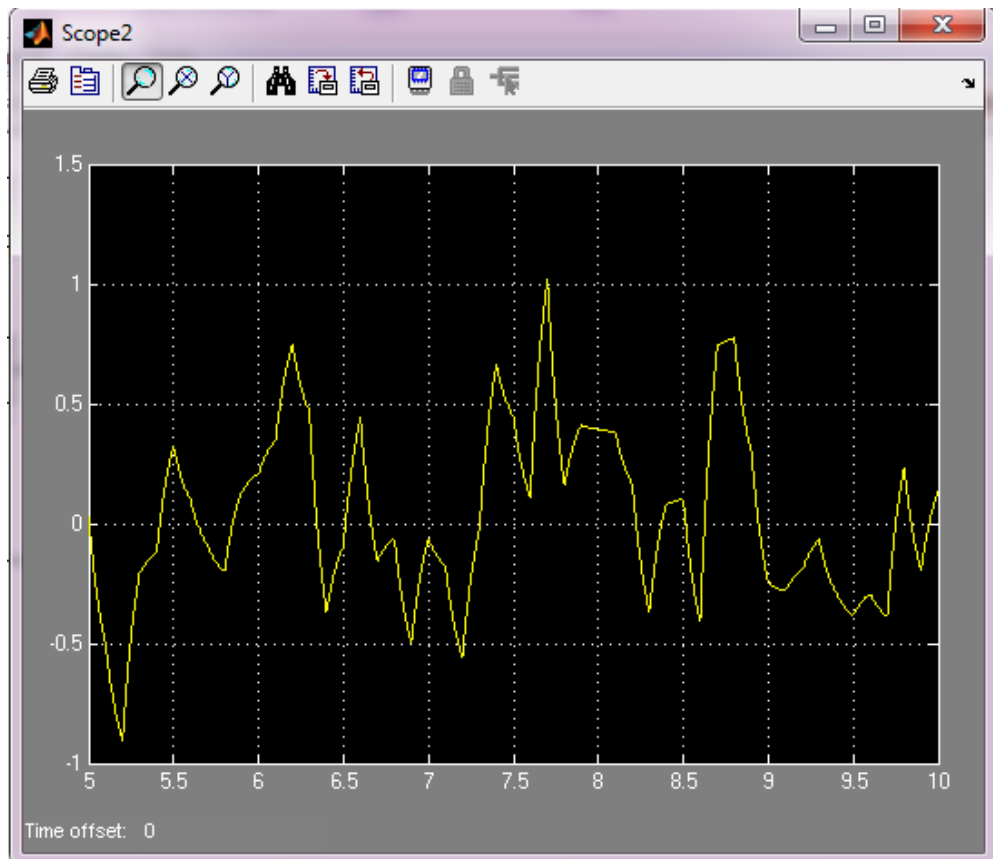


Figure 3.30: Input block parameters



Input



Output

Figure 3.31: Input/output training pattern

3.4.2 Creating and Training the Neural Network

After generating the training data, typing commands was started to create and train the neural network at MATLAB command window as **Appendix B**. To generate a simulink model of the trained neural network, the command gensim was used which is written as gensim(network name, sampling time), choose a sample time of 1e-3 for good accuracy as follow:

```
>> gensim(net,1e-3)
```

The blue NN model as figure 3.32 was copied and paste into a new simulink model to test it as a third step.

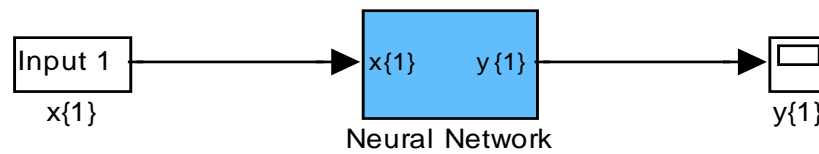


Figure 3.32: Generating simulink model of ANN Estimator

3.4.3 Testing the Trained Neural Network

In this step, the trained neural network will be tested using a testing input. A new Simulink model was build to consist of both plant model and NN model subjected to the same input as shown in figure 3.33. Use the training input as the test input or change its parameters. In this example, first option will be used. Observe the plant output and the NN model output on the same scope. If the training is good enough, the result should find the two outputs very similar as shown in figure 3.34.

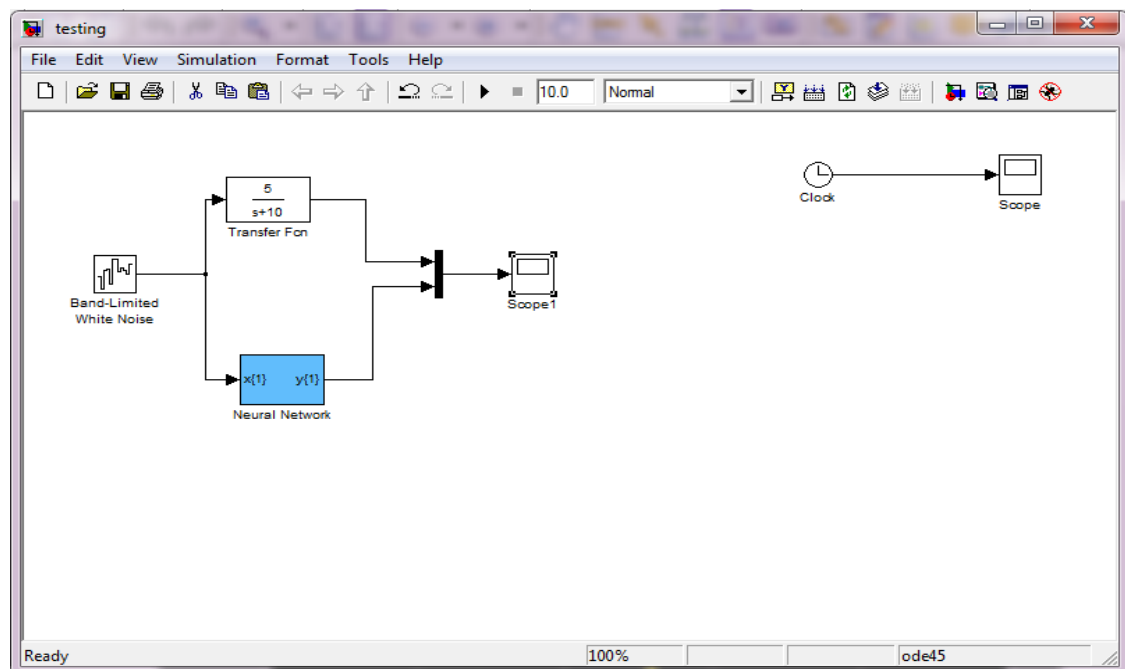


Figure 3.33: Simulink model of NN model testing

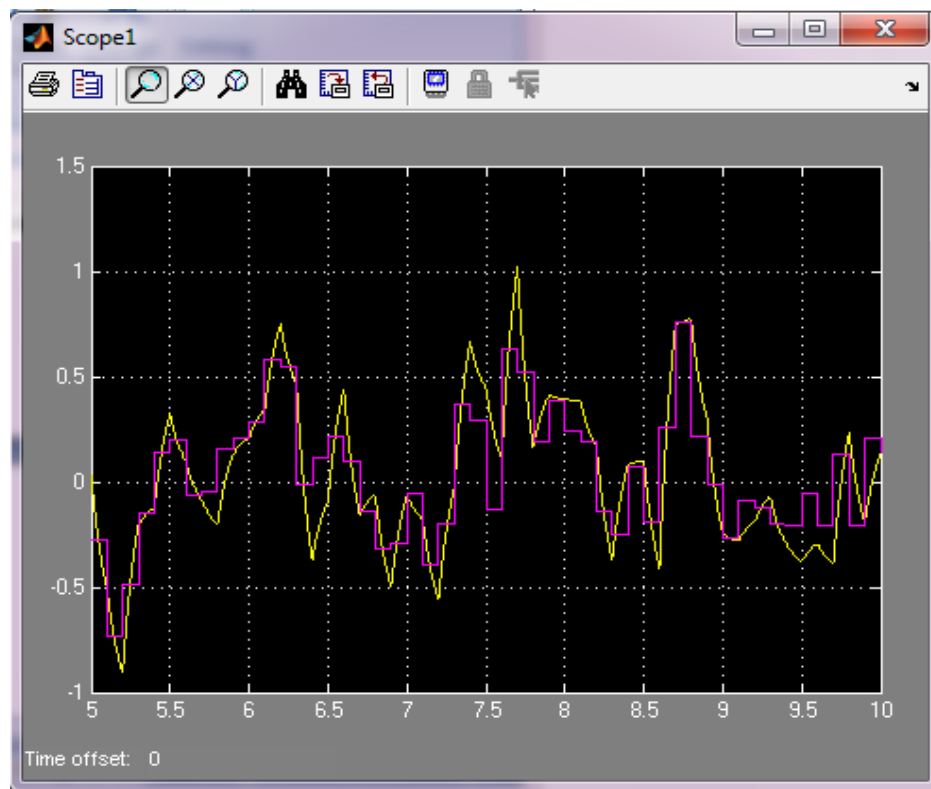


Figure 3.34: Actual plant and NN model outputs

3.5.0 Neural Network Correction

ANN have been applied in the field of diagnosis in medicine, engineering and manufacturing by correct association between input patterns representing some forms of abnormal behavior with the corresponding disease or fault type. It is fault diagnosis of electrical motors and correction will be made.

3.5.1 Development of Neural Network Correction

Correction was made at D-axis stator currents block in the estimation motor. Workspace block was added at the end of I_s output and R_s input as shown in figure 3.35. Then the workspace was double-click and the input were changed to p and the output was changed to t like in figure 3.36. The save format was changed from structure to array.

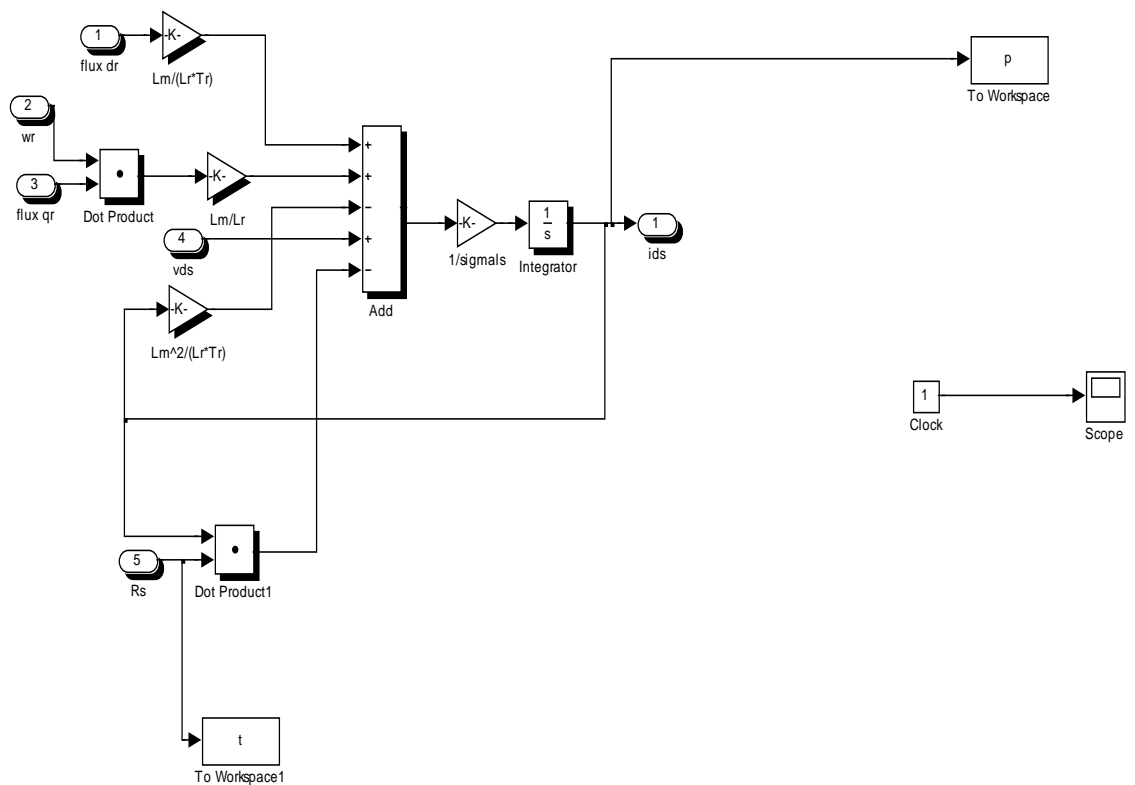


Figure 3.35: Correction simulink block

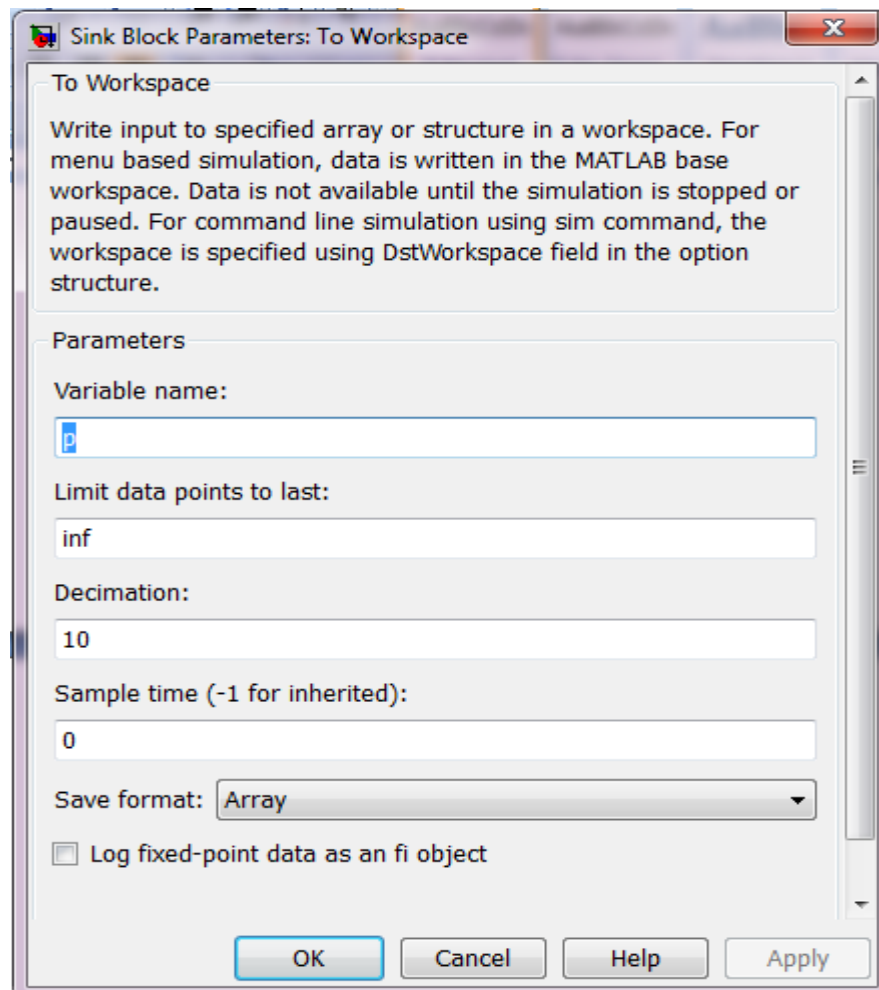


Figure 3.36: Input block parameter

After generating the training data, go to Matlab command window and start typing commands to create and train the neural network as **Appendix C**. Result will get the following figure 3.37.

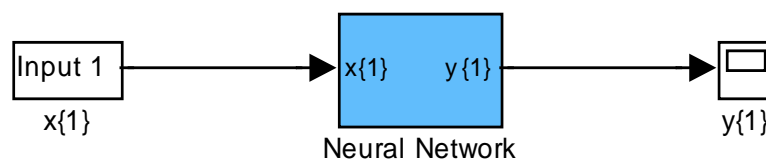


Figure 3.37: Simulink model of ANN Estimator

CHAPTER IV

RESULT & DISCUSSION

4.0 Introduction

For this project, a few results have been taken. This section consist no load, on load, and stator resistance estimation of induction motor and resistance estimation of induction motor using Neural Network.

4.1 No Load Analysis

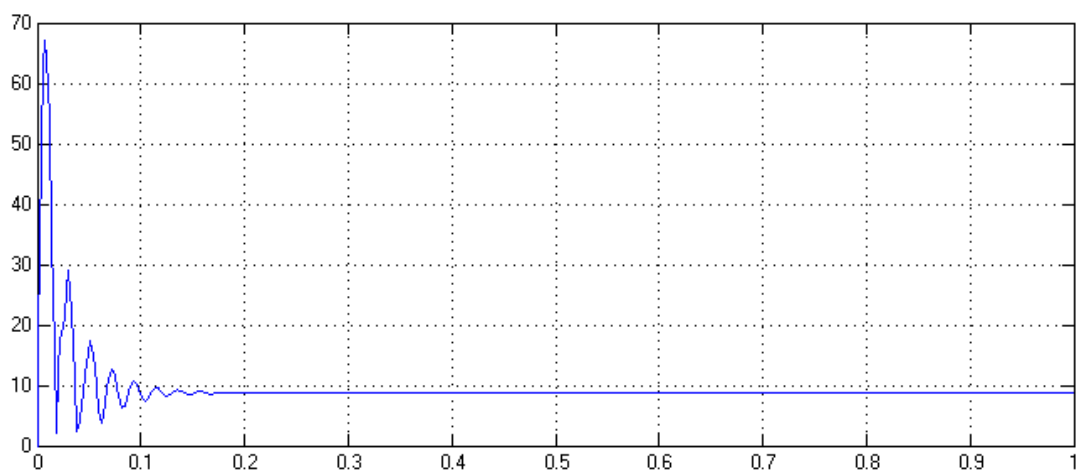


Figure 4.1: Stator Current $I_s(k)$ at no load

At 0.025, the stator current for induction motor is 68A as shown in figure 4.1. This is the maximum current achieved by induction motor cause motor need high starting current to turn on. After that, the stator decrease slowly and become stable at 0.17 second with current value is 8.5A. The current is still needed even though there is no load at induction motor. The current for no load motor is lower than on load induction motor. The induction was assumed motor without losses for this section.

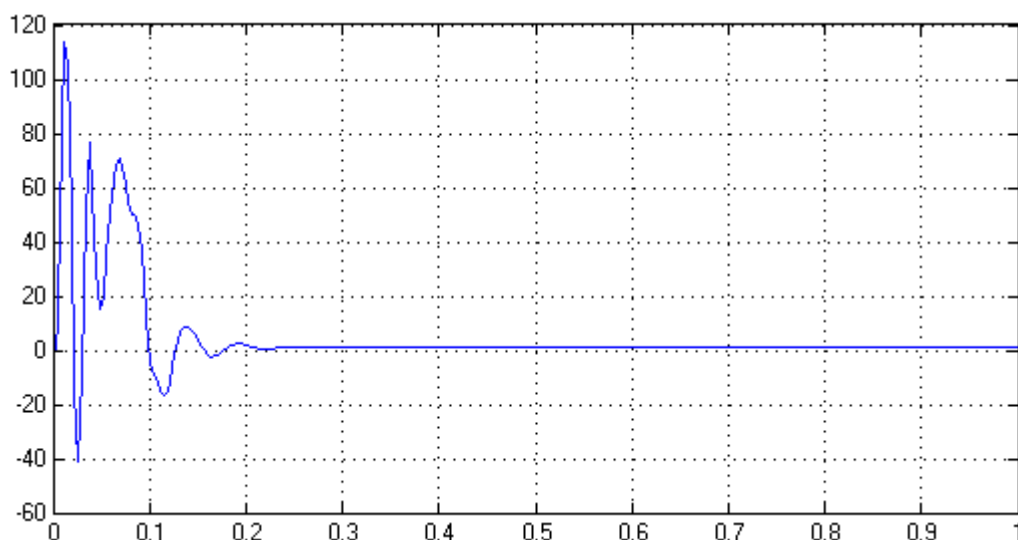


Figure 4.2: Torque at no load

In the figure 4.2 shows that the torque at no load takes time less than 0.25 second to stabilize. Induction motor use the maximum torque to start moving the rotor with value of torque is 118Nm causing starting of the graph is higher and then decreases slowly. In stabilize condition the value of synchronous speed and rotor speed is same. This theory is only suitable for motor without load.

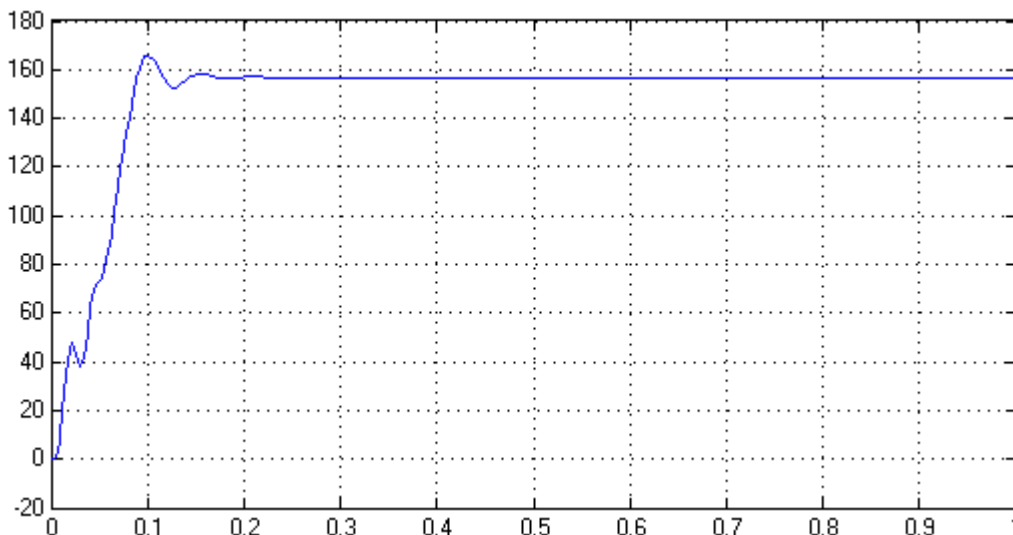


Figure 4.3: Speed of rotor at no load

The speed of the rotor increase to maximum from 0 to 0.2 and the speed are constant when the rotor rotating is stabilizing as shown in figure 4.3. In stabilize condition the value of synchronous speed and rotor speed is same. The rotor speed achieved 160.5 at 0.1 second before the speed constant.

4.2 On Load Analysis

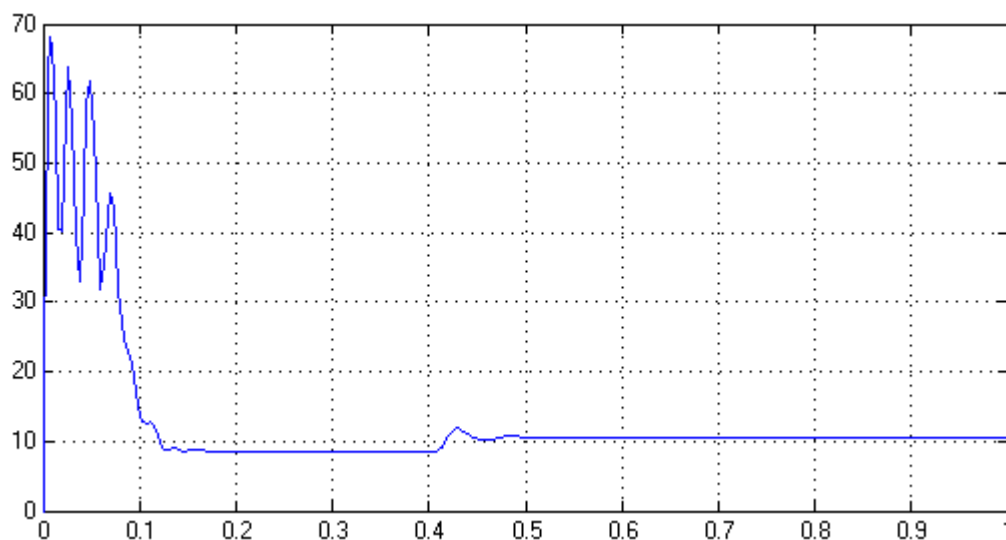


Figure 4.4: Stator Current $I_s(k)$ at on load

The maximum stator current for the on load and no load induction is same but the value current when the system is stable is different as shown in figure 4.4. This

situation occurs because more current is needed to operate the on load induction motor.

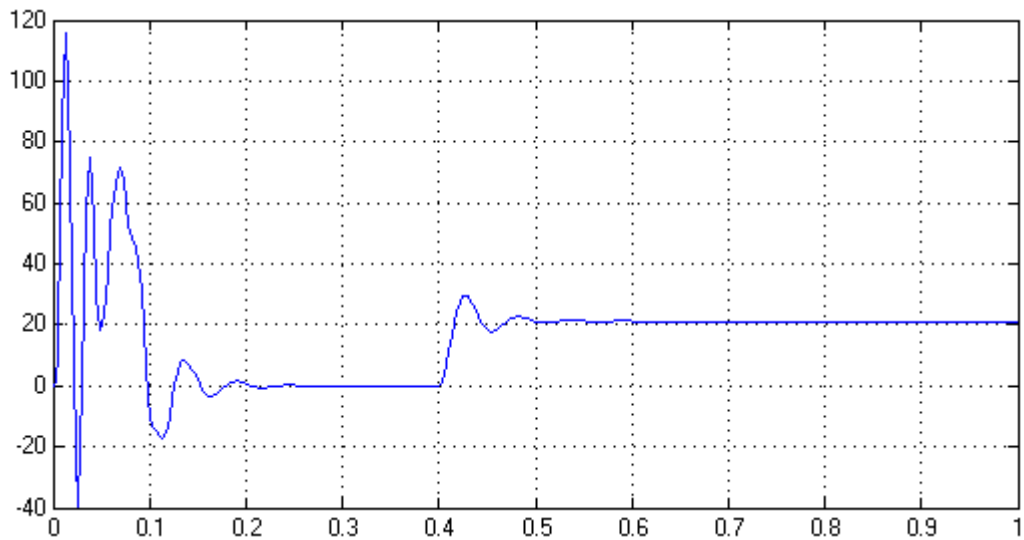


Figure 4.5: Torque at on load

In the figure 4.5 shows torque at on load take time less than 0.1 second to decrease. Induction motor use the maximum torque to start moving the rotor with value of torque is 118.0Nm causing starting of the graph is higher and then decreases slowly at 0.0Nm. Then increase to 20Nm constantly when the motor operating at stable condition. This situation happens because the motor take time to familiar with load.

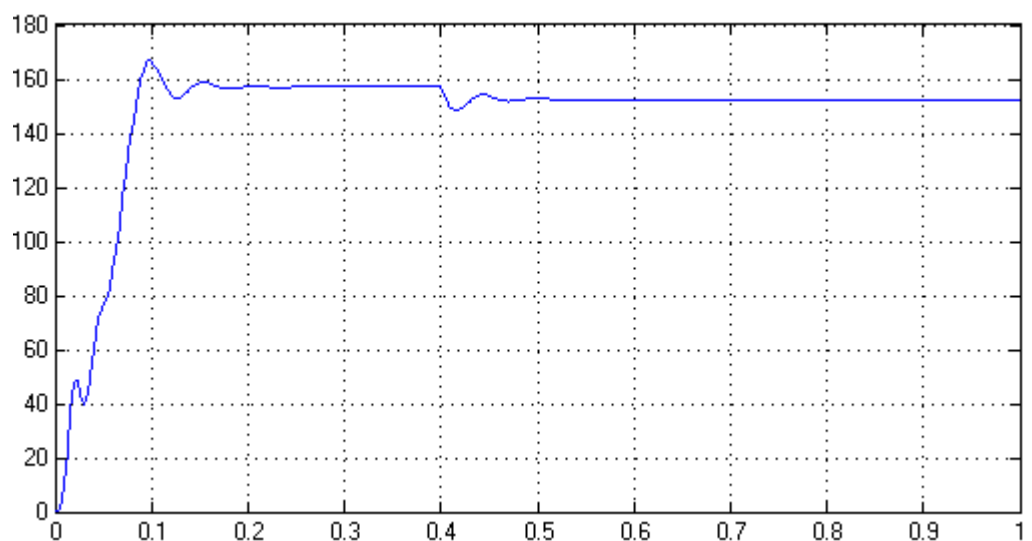


Figure 4.6: Speed of rotor at on load

The speed of the rotor increase to maximum from 0 to 0.2 and the speed is decreasing to 154.0 when the time up to 0.4 as shown in figure 4.6. For this section motor needed more time to stable when the motor has load. The speed values also decrease because the rotor needs to carry the load.

4.3 Stator Resistance Estimation Analysis

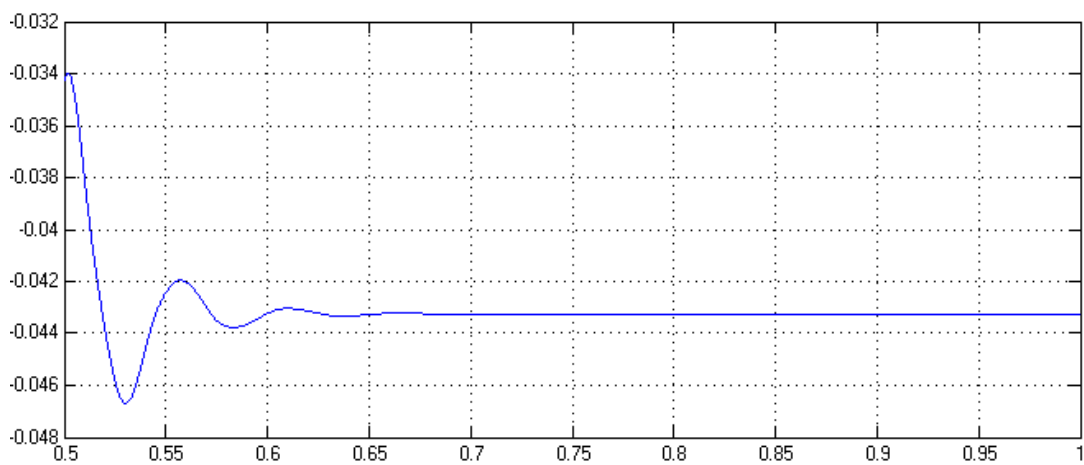


Figure 4.7: Current error between actual and estimated induction motor

Figure 4.7 shows the differences between the actual stator current with estimated stator current of induction motor. The error between the estimated stator current $I_s(k)$ and the measured stator current $I_s(k)$ is used to determine the incremental value of stator resistance (ΔR_s) through a ANN estimator

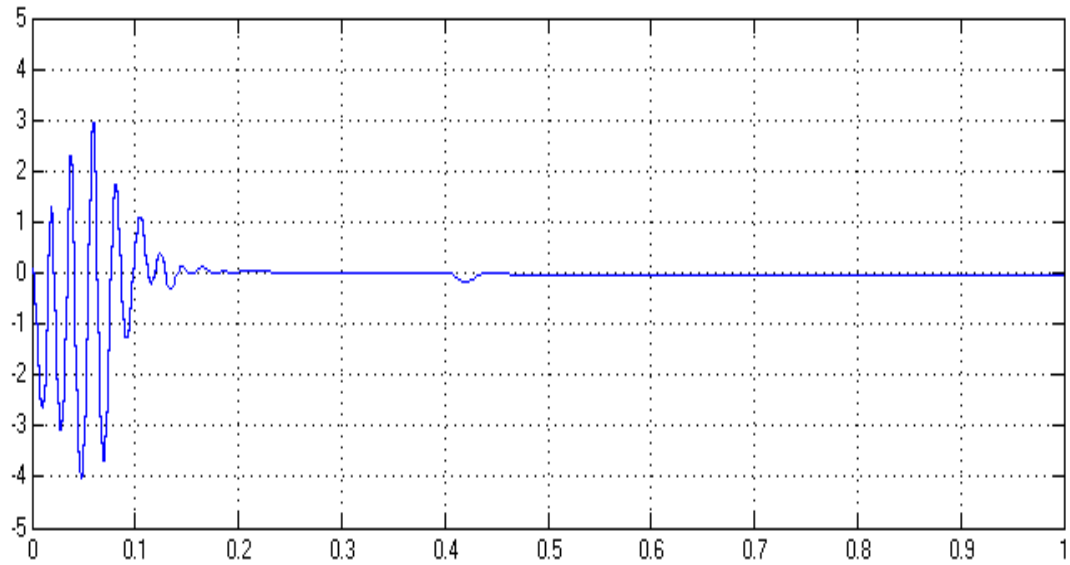


Figure 4.8: Change of stator resistance (ΔR_s).

Figure 4.8 shows the change stator resistance after (Δi_s) flow through the ANN estimator and convert to (ΔR_s).

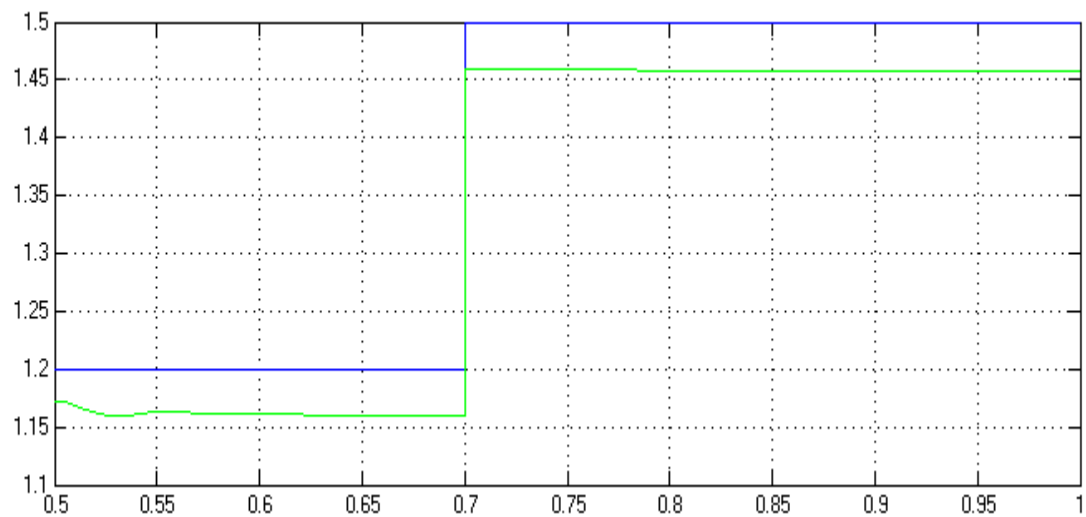


Figure 4.9: Stator resistance estimation using ANN

The green line is shows the R_s value by using ANN estimator and the blue line is actual R_s value must be estimate. Accuracy for the ANN estimator is 96.8% only. The value R_s is 1.452 as shown in figure 4.9.

4.4 Stator Resistance Correction Analysis

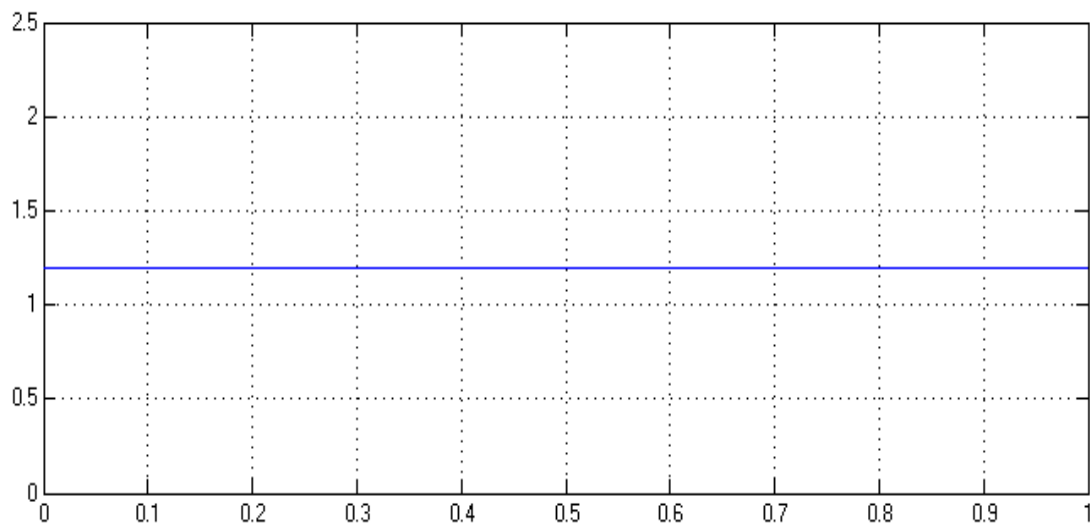


Figure 4.10: Stator resistance correction using ANN

ANN correction make adjustment from the error R_s is 1.452 to 1.2. The correction for R_s value is straight line because of using suitable value clock as in figure 4.10. Correction process is training by using actual motor R_s value.

CHAPTER V

CONCLUSION & RECOMMENDATION

5.0 Conclusion

The purpose of this final year project is to estimate stator resistance of Induction Motor Using Artificial Neural Network and made a correction in demand to improve the approach of fault detection in polyphase induction motor. Artificial intelligence is implemented to improve traditional techniques, as the results can be obtained instantaneously after it analyzes the input data of the motor where it can be accomplished without an expert.

Artificial intelligence approached can easily do difficult analysis such as pattern recognition and nonlinear system identification and control. In this project, Feedforward Backpropagation Neural Network is used to train data and analyzes the motor condition as it is the backbone of the programming development structured to conduct monitoring in an early stage to detect stator resistance fault to eliminate the hazards of severe motor faults and preventing any miserable damage. This project is successfully with all objectives achieved.

5.1 Future Recommendation

This project was successfully accomplished using Feedforward Backpropagation Neural Network where the data is obtained by the simulation that simulated using MATLAB. However the implementations need to be improved as the theoretical value and the calculated value always discriminate each other. For future recommendation, several suggestions are proposed:

- Replace the simulation model with actual motor to analyze real time theoretical data where it is time consuming.
- Conduct the data extraction via manipulating the actual three-phase motor which requires cost of application.
- Develop an ANN which can analyze the combination of several faults in one analysis which requires further studies in Neural Network

REFERENCES

1. Marian Dumitru Negrea., (2006). '*Electromagnetic flux monitoring for detecting faults in electrical machines*', Master Thesis, Helsinki University of Technology
2. 20 March 20[1]Barker, S., (2000), *Power Engineering Journal*,
3. P. Vas,(1993) *Condition Monitoring, Diagnosis and Parameter Estimation of Electrical Machines*. Oxford, U.K.: Oxford Univ. Press, 1993.
4. Thorsen, O. V., Dalva, M., (1999), '*Failure identification and analysis for high voltage induction motors in the petrochemical industry*', IEEE Transactions on Industry Applications, Vol.35, No. 4, pp. 810-818.
5. Tavner, P., Penman, J., (1987), '*Condition Monitoring of Electrical Machines*', Research studies press LTD, 1987. ISSN/ISBN: 0-86380-061-0, 302 p.
6. M.L. Sin, W.L. Soong and N. Ertugrul(2003) '*Induction machine on-line condition monitoring and fault diagnosis*'.
7. Tallam, R.M., Habetler, T.G., Harley, R.G., Gritter, D.J., Burton, B.H.,(2000), '*Neural network based on-line stator winding turn fault detection for induction motors*'
8. http://www.mathworks.com/academia/student_version/r2009a
9. M.E.H. Benbouzid,(2000) "*A Review of Induction Motors Signature Analysis as a Medium for Faults Detection*".
10. C.M. Riley, B.K. Lin, T.G. Habetler and G.B. Kliman, (1999) "*Stator Current Harmonics and their Causal Vibrations: A Preliminary Investigation of Sensorless Vibration Monitoring Applications,*".
11. Chen Qigong, A new resistance estimator applying to fuzzy-neural network, CHINESE JOURNAL OF SCIENCE INSTRUMENT.

12. Hu Gang, Xu Xue, Hu Yuwen, A fuzzy on-line observer design in direct torque control system, neural network estimator, ELECTRIC DRIVE, China, 1997.
13. Li Yan, Shao Yuexiang, Shao Shihuang, Fang Jianan. A fuzzy direct torque control system with neural network estimator, ELECTRIC DRIVE, China, 1997,
14. Luis A. Cabrera, Malik E.Elbuluk, Tuning the stator resistance of induction motors using artificial neural network, IEEE TRANSACTIONS ON POWER ELECTRIC'S.
15. Žalman, M.: Actuating devices. STU Publishing house, Bratislava, 2003.
16. Ursem, R. K.: Models for Evolutionary Algorithms and Their Application in System Identification and Control Optimization. PhD thesis, EVALife, Department of Computer Science, Univerzity of Aarhus, 2003.
17. Sekaj, I.: Evolution computations and their practice using. IRIS Publishing house, Bratislava, 2005.
18. Z. Peng and T. Fukao, "Robust speed identification for speed sensorless vector control of induction motors," *IEEE Trans. Ind. Applicat.*, vol. 30, pp. 1234-1240, Sept./Oct. 1994.

APPENDIX A: Mathematical Expressions for Estimated Induction Motor

Stator Voltage model equation

$$\begin{bmatrix} \frac{d\lambda_{dr}^{vm}}{dt} \\ \frac{d\lambda_{qr}^{vm}}{dt} \end{bmatrix} = \frac{L_r}{L_m} \left\{ \begin{bmatrix} v_{ds} \\ v_{qs} \end{bmatrix} - R_s \begin{bmatrix} i_{ds} \\ i_{qs} \end{bmatrix} - \sigma L_s \begin{bmatrix} \frac{di_{ds}}{dt} \\ \frac{di_{qs}}{dt} \end{bmatrix} \right\}$$

Stator current model equation

$$\begin{bmatrix} \frac{d\lambda_{dr}^{im}}{dt} \\ \frac{d\lambda_{qr}^{im}}{dt} \end{bmatrix} = \begin{bmatrix} -\frac{1}{T_r} & -\omega_r \\ \omega_r & -\frac{1}{T_r} \end{bmatrix} \begin{bmatrix} \lambda_{dr}^{im} \\ \lambda_{qr}^{im} \end{bmatrix} + \frac{L_m}{L_r} \begin{bmatrix} i_{ds} \\ i_{qs} \end{bmatrix}$$

Rotor flux estimations model equation for D-frame

$$\frac{L_m d\lambda_{dr}^{vm}}{L_r dt} = v_{ds} - R_s i_{ds} - \sigma L_s \frac{di_{ds}}{dt}$$

$$\sigma L_s \frac{di_{ds}}{dt} = -\frac{L_r d\lambda_{dr}^{vm}}{L_m dt} + v_{ds} - R_s i_{ds}$$

$$\frac{d\lambda_{dr}^{im}}{dt} = \left(-\frac{1}{T_r} \lambda_{dr}^{im} \right) + (-\omega \lambda_{qr}^{im}) + \frac{L_m}{T_r} i_{ds}$$

$$\sigma L_s \frac{di_{ds}}{dt} = -\frac{L_m}{L_r} \left[\left(-\frac{1}{T_r} \lambda_{dr}^{im} \right) + (-\omega \lambda_{qr}^{im}) + \frac{L_m}{T_r} i_{ds} \right] + v_{ds} - R_s i_{ds}$$

$$\sigma L_s \frac{di_{ds}}{dt} = \frac{L_m}{L_r T_r} \lambda_{dr}^{im} + \frac{L_m}{L_r} \omega \lambda_{qr}^{im} - \frac{L_m^2}{L_r T_r} i_{ds} + v_{ds} - R_s i_{ds}$$

Rotor flux estimations model equation for Q-frame

$$\frac{L_m d\lambda_{dr}^{vm}}{L_r dt} = v_{qs} - R_s i_{qs} - \sigma L_s \frac{di_{qs}}{dt}$$

$$\sigma L_s \frac{di_{qs}}{dt} = -\frac{L_m d\lambda_{qr}^{vm}}{L_r dt} + v_{qs} - R_s i_{qs}$$

$$\frac{d\lambda_{qr}^{im}}{dt} = \left(-\frac{1}{T_r} \lambda_{qr}^{im} \right) + (\omega \lambda_{dr}^{im}) + \frac{L_m}{T_r} i_{qs}$$

$$\sigma L_s \frac{di_{qs}}{dt} = -\frac{L_m}{L_r} \left[\left(-\frac{1}{T_r} \lambda_{qr}^{im} \right) + (\omega \lambda_{dr}^{im}) + \frac{L_m}{T_r} i_{qs} \right] + v_{qs} - R_s i_{qs}$$

$$\sigma L_s \frac{di_{qs}}{dt} = \frac{L_m}{L_r T_r} \lambda_{qr}^{im} - \frac{L_m}{L_r} \omega \lambda_{dr}^{im} - \frac{L_m^2}{L_r T_r} i_{qs} + v_{qs} - R_s i_{qs}$$

D-axis stator current

$$i_{ds}^*(k) = W_4 i_{ds}^*(k-1) + W_5 \lambda_{dr}^{im}(k-1) + W_6 \lambda_{qr}^{im}(k-1) + W_7 v_{ds}(k-1)$$

Q-axis stator current

$$i_{qs}^*(k) = W_4 i_{qs}^*(k-1) + W_5 \lambda_{qr}^{im}(k-1) + W_6 \lambda_{dr}^{im}(k-1) + W_7 v_{qs}(k-1)$$

Coefficients

$$W_4 = 1 + \frac{T_s}{\sigma L_s} \frac{L_m^2}{L_r T_r} + \frac{T_s}{\sigma L_s} R_s$$

$$W_5 = \frac{T_s}{\sigma L_s} \frac{L_m}{L_r T_r}$$

$$W_6 = \frac{T_s L_m}{\sigma L_s L_r} \omega_r$$

$$W_7 = \frac{T_s}{\sigma L_s}$$

The amplitude of the stator current

$$i_s^*(k) = \sqrt{i_{ds}^*(k)^2 + i_{qs}^*(k)^2}$$

APPENDIX B :ANN Estimator

```
>> net=newff(minmax(p'),[30,1],{'tansig','purelin'},'trainlm');
```

```
>> net.trainParam.epochs=1000;
```

```
>> [net,tr]=train(net,p',t');
```

TRAINLM, Epoch 0/1000, MSE 2.85796/0, Gradient 30464.9/1e-010

TRAINLM, Epoch 25/1000, MSE 0.0384398/0, Gradient 31.4321/1e-010

TRAINLM, Epoch 50/1000, MSE 0.0345469/0, Gradient 24.9989/1e-010

TRAINLM, Epoch 75/1000, MSE 0.0322424/0, Gradient 133.248/1e-010

TRAINLM, Epoch 100/1000, MSE 0.0279006/0, Gradient 9.16506/1e-010

TRAINLM, Epoch 125/1000, MSE 0.0267224/0, Gradient 43.5687/1e-010

TRAINLM, Epoch 150/1000, MSE 0.0250702/0, Gradient 3.73641/1e-010

TRAINLM, Epoch 175/1000, MSE 0.025039/0, Gradient 1.54462/1e-010

TRAINLM, Epoch 200/1000, MSE 0.0250024/0, Gradient 1.79969/1e-010

TRAINLM, Epoch 225/1000, MSE 0.0249883/0, Gradient 8.63699/1e-010

TRAINLM, Epoch 250/1000, MSE 0.0249872/0, Gradient 0.152471/1e-010

TRAINLM, Epoch 275/1000, MSE 0.024987/0, Gradient 0.00954264/1e-010

TRAINLM, Epoch 300/1000, MSE 0.024987/0, Gradient 0.0324412/1e-010

TRAINLM, Epoch 325/1000, MSE 0.024987/0, Gradient 0.0860265/1e-010

TRAINLM, Epoch 350/1000, MSE 0.0249869/0, Gradient 0.0895968/1e-010

TRAINLM, Epoch 375/1000, MSE 0.0249869/0, Gradient 0.0292589/1e-010

TRAINLM, Epoch 400/1000, MSE 0.0249868/0, Gradient 1.25556/1e-010

TRAINLM, Epoch 425/1000, MSE 0.0249865/0, Gradient 1.01611/1e-010

TRAINLM, Epoch 450/1000, MSE 0.0249862/0, Gradient 0.994071/1e-010

TRAINLM, Epoch 475/1000, MSE 0.024986/0, Gradient 1.49094/1e-010

TRAINLM, Epoch 500/1000, MSE 0.0249858/0, Gradient 5.64823/1e-010

TRAINLM, Epoch 525/1000, MSE 0.0249854/0, Gradient 8.91029/1e-010

TRAINLM, Epoch 550/1000, MSE 0.0249851/0, Gradient 3.24994/1e-010

TRAINLM, Epoch 575/1000, MSE 0.0249848/0, Gradient 1.1172/1e-010

Industrial Automation Lecture Notes – SDL – ANN 27

By Shady Gadoue, Module Leader: Dr. Damian Giaouris

Newcastle University

School of Electrical, Electronic & Computing Engineering

TRAINLM, Epoch 600/1000, MSE 0.0249846/0, Gradient 0.409848/1e-010

TRAINLM, Epoch 625/1000, MSE 0.0249844/0, Gradient 0.163045/1e-010

TRAINLM, Epoch 650/1000, MSE 0.0249838/0, Gradient 0.266647/1e-010

TRAINLM, Epoch 675/1000, MSE 0.0249837/0, Gradient 0.475013/1e-010

TRAINLM, Epoch 700/1000, MSE 0.0249836/0, Gradient 0.60567/1e-010

TRAINLM, Epoch 725/1000, MSE 0.0249835/0, Gradient 0.3998/1e-010

TRAINLM, Epoch 750/1000, MSE 0.0249833/0, Gradient 0.486509/1e-010

TRAINLM, Epoch 775/1000, MSE 0.024983/0, Gradient 2.04466/1e-010

TRAINLM, Epoch 800/1000, MSE 0.0249827/0, Gradient 1.41733/1e-010

TRAINLM, Epoch 825/1000, MSE 0.0249825/0, Gradient 0.378752/1e-010

TRAINLM, Epoch 850/1000, MSE 0.0249824/0, Gradient 1.17317/1e-010

TRAINLM, Epoch 875/1000, MSE 0.0249823/0, Gradient 0.859761/1e-010

TRAINLM, Epoch 900/1000, MSE 0.0249822/0, Gradient 0.0968464/1e-010

TRAINLM, Epoch 925/1000, MSE 0.024982/0, Gradient 10.6725/1e-010

TRAINLM, Epoch 950/1000, MSE 0.0249819/0, Gradient 0.036869/1e-010

TRAINLM, Epoch 975/1000, MSE 0.0249818/0, Gradient 2.52703/1e-010

TRAINLM, Epoch 1000/1000, MSE 0.0249818/0, Gradient 3.94388/1e-010

TRAINLM, Maximum epoch reached, performance goal was not met.

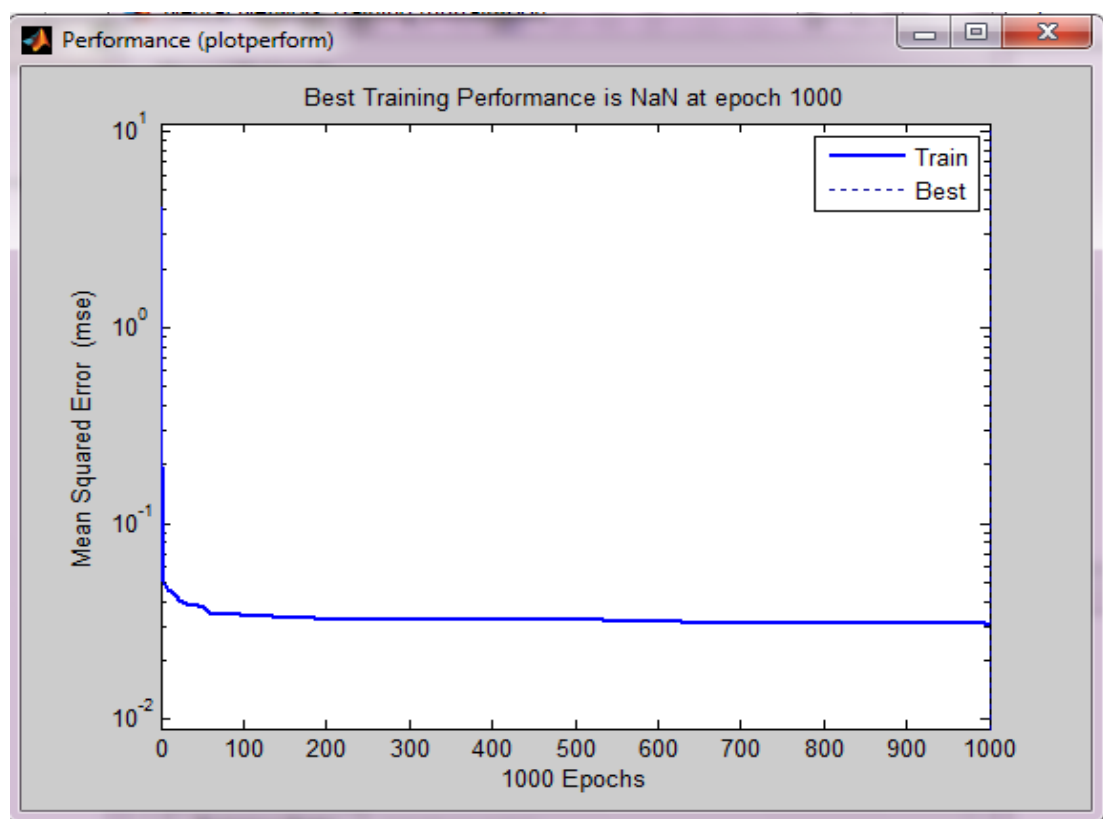


Figure 20: Network performance function during training

```
>> gensim(net,1e-3)
```

APPENDIX C: ANN Correction

```
>> net=newff(minmax(p'),[30,1],{'tansig','purelin'},'trainlm');
```

Warning: NEWFF used in an obsolete way.

```
> In nntobsu at 18
```

```
    In newff at 86
```

See help for NEWFF to update calls to the new argument list.

```
>> net.trainParam.epochs=1000;
```

```
>> [net,tr]=train(net,p',t');
```

```
>> gensim(net,1e-3):
```

APPENDIX D: Block Diagram of Stator Resistance Estimation of Induction Motor

This simulation simulates a Stator Resistance Estimation of Induction Motor Using Neural Network.

